October 2018

Evaluating the Impact of Double-Parked Freight Deliveries on Signalized Arterial Control Delay Using Analytical Models and Simulation

Aaron J. Keegan

EVALUATING THE IMPACT OF DOUBLE-PARKED FREIGHT DELIVERIES ON SIGNALIZED ARTERIAL CONTROL DELAY USING ANALYTICAL MODELS AND SIMULATION

A Thesis Presented

by

AARON J. KEEGAN

Submitted to the Graduate School of the
University of Massachusetts Amherst in partial fulfillment
of the requirements for the degree of

MASTER OF SCIENCE IN CIVIL ENGINEERNG

SEPTEMBER 2018

Civil and Environmental Engineering

EVALUATING THE IMPACT OF DOUBLE-PARKED FREIGHT DELIVERIES ON SIGNALIZED ARTERIAL CONTORL DELAY USING ANALYTICAL MODELS AND SIMULATION

A Thesis Presented

By

AARON J. KEEGAN

Approved as to style and content by:

_____

Eric J. Gonzales, Chairperson

_____

Michael A. Knodler Jr., Member

_____

Richard N. Palmer, Department Head
Civil and Environmental Engineering

DEDICATION

To family, friends, co-workers, and housemates who were supportive and encouraging during this period of my life.

ACKNOWLEDGMENTS

I acknowledge and give my sincere thanks to my research advisor, Dr. Eric J. Gonzales, for his expertise, patience, and professionalism in guiding me through this project. Additionally, my coursework with Dr. Gonzales was essential and enlightening.

I thank Dr. Michael Knodler for welcoming me into the UMass family from day one. I also thank Dr. Knodler for both his perspective on this project and his professionalism and enthusiasm as a professor and leader.

Thanks is also due to Dr. Eleni Christofa whose course material on traffic flow theory, simulation, and transportation sustainability were essential to my education and graduate school experience.

Special thanks to the New York City Department of Transportation Office of Freight Mobility for capturing and providing video data for use in this project. In particular, S. Hodge, N. Patel, and B. Abdoul Karim, who were gracious and helpful.

ABSTRACT

EVALUATING THE IMPACT OF DOUBLE-PARKED FREIGHT DELIVERIES ON SIGNALIZED ARTERIAL CONTROL DELAY USING ANALYTICAL MODELS AND SIMULATION

SEPTEMBER 2018

AARON J. KEEGAN, B.A., WARREN WILSON COLLEGE

B.S.C.E., WASHINGTON UNIVERSITY IN ST. LOUIS

M.S.C.E., UNIVERSITY OF MASSACHUSETTS AMHERST

Directed by: Professor Eric J. Gonzales

Freight deliveries on signalized urban streets are known to cause lane blockages during delivery. Traffic congestion associated with urban freight deliveries has gained increasing attention recently as traffic engineers and planners are tasked with finding solutions to manage increasing demand more sustainably with limited road capacity. The goal of this research is to evaluate two models for quantifying the capacity and signalized control delay effects of a lane-blocking freight delivery on an urban arterial. The two methods are: an All-or-Nothing model similar to methodology used in the Highway Capacity Manual 6th Edition, and a Detailed model consistent with kinematic wave theory. The purpose is to provide insight on the use of these tools for analysis of urban freight delivery. The signalized control delay results of the two models are compared with observed video data of urban deliveries from one city block of 8th Ave in New York City. Empirical confirmation of double-parked delivery impact on signalized controlled delay remains elusive due to an inability to isolate the effects of the deliveries from other traffic perturbations in the video sample. Instead, microscopic simulation using Aimsun is used for comparison to the theoretical models and the results lend credibility to the Detailed model. The simulation results show a similar trend of delay impact from double-parked deliveries located at a range distances from the intersection and more closely resembled the Detailed model. The All-

or-Nothing model would provide only a coarse representation of the capacity and delay effects. The more detailed approach that accounts for the dynamics of queuing in front of the delivery vehicle provides closed form analytical formulas for capacity and signalized control delay that can account for varying locations of deliveries as well as analysis periods with some blocked cycles and others unblocked. Two policy implications are proposed: 1) that double-parked deliveries located mid-block likely result in less signalized control delay impact, and 2) freight receivers that attract double-parked deliveries near an intersection stop line should be prioritized in urban freight delivery mitigation policies such as off-hour delivery.

TABLE OF CONTENTS

Page

LIST OF TABLES

Table Page

LIST OF FIGURES

Figures Page

CHAPTER 1

INTRODUCTION AND EXISTING METHODOLGY

1.1 Introduction

Freight deliveries are known to disrupt traffic on urban arterials. Traffic congestion associated with urban freight deliveries has gained increasing attention in recent years as traffic engineers and planners are tasked with finding solutions to manage increasing demand in a more sustainable way with limited road capacity. Although trucks make up only a small percentage of vehicular traffic (6% of vehicles on urban freeways), they incur a greater proportion of the total cost of delays (26% of total cost) (1). In the U.S., approximately 7% of urban traffic is made up of trucks (2), but the deliveries are increasing dramatically because of growth in e-commerce. Current urban freight policies, e.g. off-hour delivery programs, are intended to mitigate the impacts on traffic congestion.

This study presents an analysis using traffic flow theory and microsimulation to quantify the effect of double-parked urban freight deliveries on the signalized control delay experienced by traffic on an urban arterial street segment. Although there is an increasing body of literature related to policies and operational issues associated with urban freight movements, there is a need for systematic analysis of the localized impact of individual deliveries on traffic.

1.2 Literature Review

The effects of truck deliveries in urban networks can be generally separated into two categories: 1) the effect of heavy vehicles in the traffic stream on the flow of vehicles, and 2) the effect of truck delivery stops on traffic flow when lane blocking occurs. The first category of effects has been analyzed more extensively in the literature. Some studies have made use of

traffic simulations to account for the effect of trucks in the traffic stream (3, 4). Other studies have made use of empirical field measurements along with calibrated traffic simulations (5). A significant synthesis of the effects of heavy vehicles in the traffic stream was published in NCFRP Report 31 (6). The report summarizes the effect of trucks on mid-block arterial speeds and presents improved methods for calculating truck passenger car equivalent factors for capacity analysis of signalized intersections. These methods do not account for blockages caused by parked trucks.

The effect of freight delivery stops that block lanes of traffic on arterial capacity and intersection delays has received less attention in the literature. Han et al. (7) conducted a GIS-based investigation of the extent and order of magnitude of double-parking disruptions for pickups and deliveries nationwide in the U.S. Other recent studies have considered the problem of truck parking for deliveries from the perspective of the carrier (8–10). Others have identified many of the characteristics of delivery patterns and businesses on urban streets (11, 12). Very few investigations of the effect of parked trucks on intersection capacity have been conducted, and they have not provided a comprehensive analytical approach for estimating capacity and signalized control delay impacts (13).

A growing body of research has investigated policies to encourage the schedule of deliveries in urban areas during off-peak hours (14–17). Although a major motivation for off-hour delivery programs is to reduce traffic congestion, much of the analysis focuses on the experience from the perspective of the delivery drivers, who are able to travel at greater speeds during lower traffic periods (18–20). The challenge is to convince receivers to schedule off-hour deliveries, which could require paying an employee of a store to stay after normal business hours or make special arrangements for the delivery to be made in the absence of someone to receive the delivery (21). Programs to reduce traffic congestion by managing urban freight exist(22, 23). A trial off-peak delivery program in New York City paid businesses

approximately $2,000 to receive shipments during off-hours rather than normal business hours for a month; carriers were paid $300 to participate in the trial (24). Evaluations of the congestion and reliability effects of the off-hour delivery program in New York required extensive simulation analysis and considered macro-scale traffic congestion but did not include the impact of lane blocking during delivery (4,25). Being able to quantify the effects of double-parked urban freight deliveries on the performance of signalized streets in terms of delay would be useful for evaluating urban freight delivery policies that may attempt to reduce, relocate, or reschedule urban freight deliveries.

1.3 Study Contribution

The intended contribution of this study is to call attention to the impact of double-parked delivery vehicles on signalized control delay for consideration in urban freight policy. The study develops and analyzes two analytical models to quantify the impact of double-parked delivery vehicles on the signalized control delay of an urban street segment consistent with kinematic wave theory (26, 27). The Highway Capacity Manual 6th Edition (28), referred to here as HCM6, does not include guidance on double-parked urban freight deliveries. This study proposes a methodology, the Detailed model, for incorporating double-parked delivery impact on signalized control delay during the analysis of an urban street facility.

1.4 Existing Highway Capacity Methodology

This section describes in brief how the HCM6 accounts for delay on an urban street segment. The incorporation of lane blockage events in the HCM6 are discussed here to provide context and comparison between the HCM6 and analytical models presented later that estimate the effect of a double-parked delivery vehicle on the signalized control delay of an urban street segment. The HCM6 does not include methodology to account for the effect of double-parked delivery vehicles, a limitation which is explicitly noted in the HCM6 text.

1.4.1 Background on Urban Street Segments

The HCM6 is a state of the practice publication for traffic engineers and transportation planners which includes methods for the analyses of mobility on urban street facilities from the perspective of motor vehicle drivers among other modes. Urban arterials and collectors are typical examples of urban street facilities which are evaluated in the HCM6 as a series of segments. The boundaries of the segments are typically determined from intersecting cross streets or intersection controls. Urban street facilities are evaluated by aggregating the performance measures on a series of segments that make up the facility. Each individual segment consists of a link, the travel lanes of the segment, and a point, the downstream intersection of a segment. The concept of lane groups is employed to aggregate adjacent lanes that are identical and isolate lanes that serve a unique movement or set of shared movements. The lane groups are evaluated separately, and then a combined weighted performance measure is calculated for the whole street segment approach to the downstream intersection. Level of service is one of the key operational performance measures evaluated on each segment which considers both delay in running time on the link portion of the segment and delay at the downstream intersection of the segment. This study focuses exclusively on delay at the intersection.

Various sources of vehicle delay on a street segment are incorporated into the methodology, for example: street geometry, land use, other travel modes, heavy vehicles, and parallel parking. The pick-up and delivery activity of freight vehicles are not included in the methodology as a source of urban street segment delay with respect to either running time or signalized control delay. Furthermore, there is no procedure for accounting for delay that arises from vehicles changing lanes to avoid a double-parked delivery vehicle. The HCM6 limitations with respect to delivery vehicle activities are explicitly noted in the text in Chapters 17 and 18. The HCM6 also notes that if additional sources of delay are present on the urban street segment

under analysis, the analyst may attempt to include them in the methodology, particularly if operational observations have been made.

1.4.2 Lane Blockages Resulting from Parallel Parking and Bus Stopping

Parallel parking maneuvers and buses stopping in travel lanes are two types of lane blockage events contributing to signalized control delay on an urban street segment that are included in the HCM6. In both cases an adjustment factor is created to reduce the saturation flow rate of the affected lane groups for the duration of the whole analysis period. Both adjustment factors assume that the travel lane is effectively unavailable to vehicles during the time that the lane is blocked, thereby lowering the average lane capacity during the analysis period.

The adjustment factor for parallel parking is applied when a parking area is located adjacent to a travel lane, on either shoulder, within 250ft of the downstream stop line. The factor accounts for both the frictional effect of parked vehicles on the shoulder and an assumed 18 second lane blockage per parallel parking maneuver. An upper limit of 180 parking maneuvers per lane group per hour is established. The equation for the parking adjustment factor is found in the HCM6 as:

$$f_p = min\left\{\frac{N - 0.1 - \frac{18N_m}{3600}}{N}, 0.050\right\}, \quad (1)$$

where f_p is the parking adjustment factor, N_m is the parking maneuver rate adjacent to the lane group, and N is the number of lanes in the lane group.

The adjustment factor for buses stopping in travel lanes, $f_{bb,}$ is used to reduce the saturation flow rate of a lane group when buses are observed to stop in the lane at a near-side (upstream) or far-side (downstream) location within 250 ft relative to the intersection stop line under evaluation. An upper limit of 250 buses per hour is suggested. A duration of 14.4 seconds

of lane blockage time is assumed per bus stop. The equation for the bus-blockage is found in the HCM6 as:

$$f_{bb} = min\left\{\frac{N - \frac{14.4N_b}{3{,}600}}{N}, 0.050\right\}, \quad (2)$$

where f_{bb} is the bus-blockage factor, N is the number of lanes in the lane group, and N_b is the number of stopped bus events in the lane group.

1.4.3 Work Zones and Lane Restrictions

For the first time, the HCM6 contains methodologies for incorporating the effects of work zones and downstream lane blockages on urban street segments. One method, a factor for downstream lane blockages, considers the effect of downstream mid-segment lane blockages on the closest upstream intersection. The applicable mid-segment lane blockages are described as work zones, traffic incidents, or similar events. By creating a factor to reduce saturation flow rate, the methodology ensures that the capacity of movements exiting the upstream intersection cannot exceed the capacity at the location of the downstream lane blockage. The capacity of the downstream lane blockage is found in the HCM6 as:

$$c_{ms} = min\{0.25k_j N_{unblk} S_f, 1800N_{unblk}\}, \quad (3)$$

where c_{ms} is the mid-segment capacity at the site of the downstream restriction, k_j is the jam density per lane, N_{unblk} is the number of open lanes where the restriction is located, and S_f is the free-flow speed. The adjustment factor for downstream lane blockage is then found in the HCM6 as:

$$\text{If } c_{ms} < c_i \text{ or } f_{ms,i-1} < 1.0, \text{then } \; f_{ms,i} = min\left\{ f_{ms,i-1}\frac{c_{ms}}{c_i}, 0.1\right\},$$
$$\text{otherwise } \; f_{ms,i} = 1.0, \quad (4)$$

where $f_{ms,i}$ is the adjustment factor for a downstream mid-segment lane blockage and c_i is the capacity of the movement entering the blockage location. The subscript, *i*, refers to the iterative process set forth in the urban street segment methodology whereby total segment arrival volumes and lane group volume allocations are balanced in an iterative process. As for the location of the downstream lane restriction, the HCM6 says only qualitatively that the closer a downstream lane restriction is to an upstream intersection, the greater the impact on the intersection. In summary, the mid-segment lane blockage factor imposes the capacity constraint of a downstream bottleneck on the discharge capacity of the upstream intersection but does not delve into the dynamics of traffic flow around the downstream lane restriction.

The work zone presence adjustment factor is the second example of a lane restriction methodology included in the HCM6 for the first time. Whereas the factor for downstream lane blockage is used to reduce the traffic flow exiting an upstream intersection, the work zone presence adjustment factor is used to adjust the saturation flow rate on a segment where a work zone is located. The work zone is considered to be on an intersection approach if any part of it is located within 250ft of the downstream stop line. The factor can be applied if the work zone is located on the shoulder or if it blocks one or more lanes. The following equations are found in the HCM6 to calculate the work zone adjustment factor:

$$f_{wz} = min\{0.858 * f_{wid} * f_{reduce}\ , 1.0\} \tag{5}$$

with

$$f_{wid} = \frac{1}{1 - 0.0057(a_w - 12)} \tag{6}$$

and

$$f_{reduce} = \frac{1}{1 + 0.0402(n_o - n_{wz})} \tag{7}$$

where f_{wz} is a adjustment factor for work zone presence, f_{wid} is an adjustment factor for approach width, f_{reduce} is the adjustment factor reducing lanes during work zone presence, a_w is the approach lane width of all open lanes at the work zone location, n_o is the number of left turn and through lanes open during normal operation, and n_{wz} is the number of left-turn and through lanes open during work zone presence. The most restrictive cross section of open lanes adjacent to the work zone is used to calculate the work zone adjustment factor.

Both the mid-segment lane blockage factor, and the work zone presence factor limit the saturation flow rate at the site of the blockage to something less than the full saturation flow rate of the available open lane width(s), meaning the factors impose a frictional effect on the remaining open lanes. An explanation for this is that work zones are often signed with warnings and or contain moving equipment or workers that cause traffic to further slow. As for traffic incidents, an emergency responder may be present and passing vehicles may slow to look at the incident. Lastly, it should be noted that the work zone presence adjustment factor does not allow for the possibility that a lane blocked by the work zone could be partially open downstream of the work zone allowing vehicles to use the lane near the stop line.

1.4.4 Sustained Spillback on an Urban Street Segment

If a downstream urban street segment with or without a lane restriction is found to experience sustained queue spillback onto an upstream segment during the analysis period, the HCM6 contains a method to create a spillback adjustment factor that encompasses the previously described mid-segment lane blockage factor. The full spillback analysis procedure is lengthier than is warranted to describe in detail here, as it involves the division of the analysis period into smaller time periods and the determination of origin and destination movements on the segment. However, the overall concept is the creation of a spillback factor that reduces the saturation flow rate of traffic movements from the upstream segment so that they are balanced with traffic exiting the downstream segment where the sustained queue spillback has occurred. Insofar as the

downstream segment is constrained by all saturation flow rate adjustment factors that are applicable, activity reducing saturation flow on the downstream intersection is also constraining the upstream intersection using the sustained spillback analysis procedure.

1.4.5 Urban Street Facility Reliability

An evaluative procedure for urban facility reliability appears for the first time in the HCM6. The reliability procedure draws upon the methodology provided for urban facility analysis and calls for the creation of a set of plausible scenarios that attempt to map out the universe of likely conditions and incidents that can be expected on the urban facility. As noted in the HCM6, because a double-parked delivery vehicle is not included in the urban street segment methodology, it is also inherently not included in the procedure for estimating urban facility reliability. The HCM6 makes a point to mention that regularly recurring incidents that individually have a moderate impact on facility delay tend to have a larger impact on annual facility delay compared to infrequently occurring incidents that have a large impact on delay individually.

1.4.6 Capacity and Delay for a Signalized Urban Street

In this section we will look at the HCM6 evaluation of capacity and delay on a simple urban street segment operating with no lane restriction. We consider a one-way, two-lane urban street segment controlled by a pre-timed signal at the downstream intersection. The street segment has two lane groups: a lane group for through vehicles and another lane group for shared right-turns. A diagram of the urban street segment is shown in Figure 1.

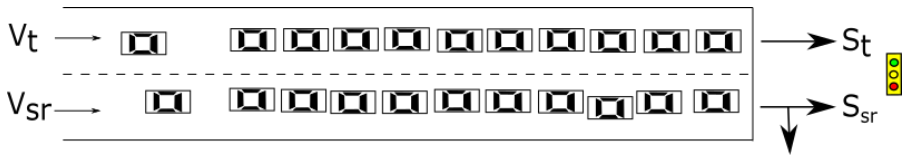

Figure 1: A Simple Two-Lane Urban Street Segment

The two-lane groups have different saturation flow rates where S_{sr} is the saturation rate for the shared right-turn lane and S_t is the saturation rate of a through lane. The arrival volumes v_t and v_{sr}, in units of vehicles per hour, are calculated using an iterative method from Chapter 31 in the HCM6 which balances the lane group arrival volumes for through moving vehicles proportionally with the lane group saturation flow rates.

Each lane group's capacity is calculated based on the saturation flow rate and signal phasing. For a pre-timed traffic signal with no permitted left turns, the capacity of the through lane, c_t, and the capacity of the shared right-turn lane, c_{sr}, are found in the HCM6 as:

$$c_t = s_t N_t g/C \tag{8}$$

$$c_{sr} = s_{sr} N_{sr} g/C \tag{9}$$

where N_t is the number of lanes in the exclusive through lane group, N_{sr} is the number of lanes in the shared right-turn lane group, g is the effective green time, and C is the cycle length. For a lane group with no permitted turning movements, the uniform control delay at the intersection is calculated using the following HCM6 equations:

$$d_1 = PF \frac{0.5C(1 - g/C)^2}{1 - (\min\{1, X\}\, g/C)} \tag{10}$$

with

$$PF = \frac{1-P}{1-\frac{g}{C}} * \frac{1-y}{1-\min(1,X)\,P} * [1 + y\frac{1-\frac{PC}{g}}{1-\frac{g}{C}}] \quad (11)$$

and

$$y = \min(1,X)\,g/C \quad (12)$$

where d_1 is uniform control delay, PF is a progression adjustment factor, P is the proportion of vehicles arriving during green indication, X is the volume-to-capacity ratio, and y is the flow ratio. The delay for each lane group is then weighted by lane group arrival volume to calculate an overall approach delay.

The Queue Accumulation Polygon (QAP) method is another delay calculation method in the HCM6 which must be used when an approach includes permitted turning movements or if there is a residual queue at the end of the signal cycle. The QAP method is introduced here, because it will later allow better visualization of the delay calculations when a freight delivery causes a lane blockage.

Figure 2 shows an example QAP diagram for the through lane group of the simple two-lane street segment. The number of vehicles in queue grow during the red phase, reaching a maximum queue length in vehicles denoted by Q_1 and receding during the green phase. The arrival flow is denoted by q_t, in vehicles per second, because the QAP shows a single signal cycle in units of seconds.

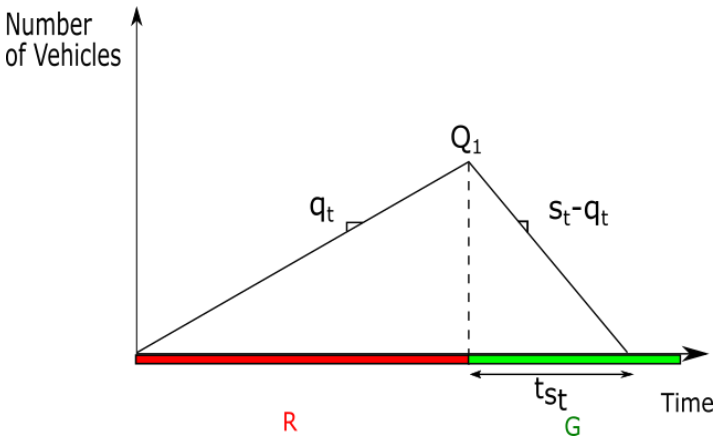

Figure 2: A Queue Accumulation Polygon of Uniform Control Delay

An important characteristic of queuing at the intersection is the maximum extent of the queue in distance from the stop line at a given arrival rate. In Figure 2, the time it takes for the queue to clear after the signal turns green, t_{s_t}, is given by:

$$t_{s_t} = \frac{q_t(C-g)}{s_t - q_t}. \tag{13}$$

The calculation of the length of queue follows from the geometry of the figure, and it can be expressed in units of distance as x_{BQ}, from the intersection stop line by dividing by the number of lanes N and the jam density of vehicles per distance k_j in the equation:

$$x_{BQ} = \frac{q_t(C-g+t_{s_t})}{Nk_j}. \tag{14}$$

When the arrival rate of a lane group fully saturates the intersection, the location of the back of the queue will be denoted here as x_{gmax}, which is obtained by evaluating eq. 14 when the value of q_t is such that $t_{s_t} = g$. The distance x_{gmax} is the longest length of queue that can be served in a lane group during the green time.

The total delay of a lane group is the sum of uniform control delay, incremental delay, and initial queue delay given by the HCM6 equation:

$$d_t = d_1 + d_2 + d_3 \tag{15}$$

where d_t is total delay, d_1 is the uniform control delay, d_2 is the incremental delay, and d_3 is the initial queue delay.

The uniform control delay is calculated as the area bounded within the constructed QAP diagram. The polygon is subdivided into intervals defined by when either the arrival flow rate or discharge rate of the lane group changes within a signal cycle. The interval length is the base of the triangle or trapezoid, while the height of each interval is given by the peak queue length. A general form equation for delay using the QAP method is found in the HCM6 as:

$$d_1 = \frac{0.5\sum_{i=1}(Q_{i-1} + Q_i)t_{t,i}}{qC} \tag{16}$$

where Q_{i-1} is the queue length of the prior interval, and Q_i is the queue length of the current interval i, $t_{t,i}$ is the time duration of interval i, and other variables are as previously defined.

The incremental delay component accounts for delay due to random fluctuations in demand and sustained oversaturation. The incremental delay is found with the HCM6 equation:

$$d_2 = 900\,T\left[(X_A - 1) + \sqrt{(X_A - 1)^2 + \frac{8kIX_A}{c_A T}}\right] \tag{17}$$

with

$$I = min\{1.0 - 0.91X_u^{2.68}, 0.090\} \tag{18}$$

where T is the duration of the analysis period, X_A is the average volume to capacity ratio of the lane group, c_A is the average capacity for the lane group, k is a signal control constant with a value of 0.50 for pretimed signals, I is the upstream filtering adjustment factor, and X_u is the weighted volume-to-capacity ratio for all upstream movements contributing to the volume on the

subject movement group. During undersaturated conditions, when there is no initial queue, X_A is equal to the volume to capacity ratio X, and c_A is equal to the lane group capacity c. This analysis focuses exclusively on undersaturated conditions, meaning there is no initial queue at the start of a signal cycle, therefore d_3 is equal to zero in eq. 15.

In the next section, observations of double-parked delivery vehicles are made for comparison to the implied traffic behavior in existing HCM6 methodology that treats lane blockages such as stopped buses etc. as though they eliminate the vehicular capacity of the entire lane.

CHAPTER 2

OBSERVATIONS OF URBAN FREIGHT DELIVERY

2.1 Video Data from 8th Avenue in NYC

Recorded video data from an urban street segment in Manhattan was shared with the authors by the New York City Department of Transportation Office of Freight Mobility[1]. The video data consisted of continuously recorded traffic footage between 10:30am and 4:30pm on Tuesday, August 11, 2015. The recording was made from a camera mounted on a traffic signal mast at 8th Ave and 36th St. The camera viewed 8th Ave northbound including the downstream intersection of 8th Ave and 37th St. Figure 3 illustrates the lane geometry of the 8th Ave segment and the positioning of the camera for data collection.

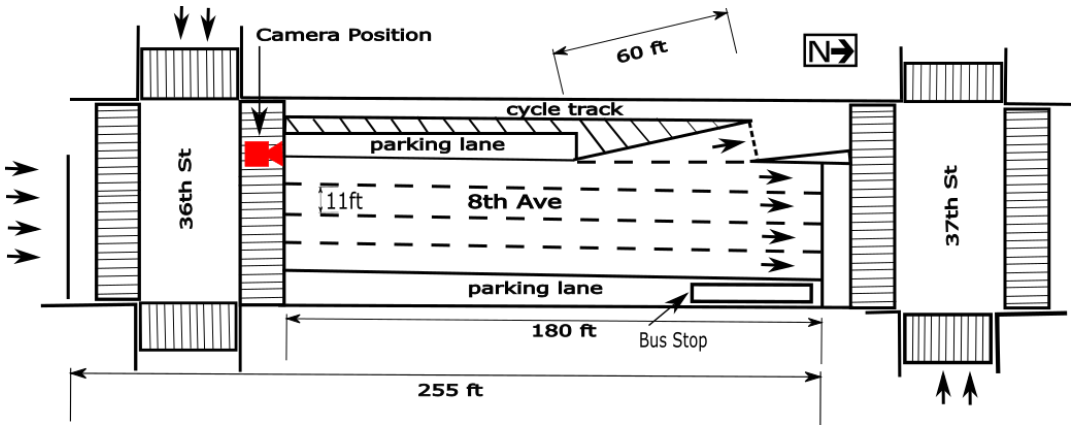

Figure 3: Diagram of 8th Ave Between 36th St and 37th St

The segment of 8th Ave under analysis is just over 180ft in length from the downstream stop line to the upstream intersection, it has four one-way northbound lanes, a diagonally oriented left turn bay that stores one or two vehicles, and parallel parking spaces on both sides. It should be noted that the through lane closest to the left curb was observed to function as a shared left-turn lane in practice despite being designated by road markings as a through lane only. Parking is restricted on the right curb near the stop line for a bus stop. The cross street at the downstream

[1] The website of the NYCDOT Office of Freight Mobility is http://www.nyc.gov/html/dot/html/motorist/trucks.shtml

intersection, 37th St, is one-way in the westbound direction and has two lanes. There is a cycle track between the left-side parallel parking bay and the sidewalk curb. The signal control is pre-timed, and all lanes have an 84 second cycle with 45seconds of green time. The signal control is coordinated with upstream and downstream segments of 8th Ave by a 6 second offset. Figure 4 shows an image of the recorded data vantage point looking north on 8th Ave during a lane blocking delivery event. The video was analyzed manually as summarized in the next section.

Figure 4: Vantage Point of 8th Ave Video Data: Looking North to 37th St

2.2 Observed Results of Double-Parked Delivery Characteristics

The segment of 8th Ave between 36th St and 37th St was very busy with delivery activity. During the six-hour observation period, there were 14 instances of delivery vehicles double-parking and blocking a lane. During the same period there were an additional 20 delivery vehicles which were able to secure a parallel parking space on a side of the street to conduct delivery activity of either a good or a service.

Table 1 summarizes the locations of the observed double-parked delivery events on 8th Ave between 36th St and 37th St. The distances from the stop lines are given between the stop line and the front of the delivery vehicle. The most frequent location for a lane-blocking delivery

vehicle was at the stop line in the left turn bay, effectively blocking the entire bay. The next most frequent location was the blockage of a through lane in the mid-block area of the street, between 60ft and 120ft upstream from the stop line. Mid-block delivery vehicles were as likely to park on the left side as the right side. Lane blocking delivery events were also observed near the upstream intersection greater than 120ft upstream from the stop line. Clearly, delivery vehicles will use a variety of locations on the street when blocking a lane to conduct delivery activity.

Table 1: The Location of Observed Double-Parked Deliveries on 8th Ave

Location Description	Vehicle Distance from stop line	Right Side of Street	Left Side of Street	Total Lane Blocking Deliveries
Left Turn Lane	0-5ft	-	6	6
Stop Line to Mid-Block	0-60ft	-	-	0
Mid-Block	60-120ft	3	3	6
Mid-Block to Upstream Intersection	120-180ft	2	-	2
Total		**5**	**9**	**14**

Figure 5 shows a chart of delivery duration vs. delivery start time for the 14 observed double-parked deliveries. The chart shows that double-parked delivery events occurred throughout the observation period, no predominant time of day clustering was evident from the sample.

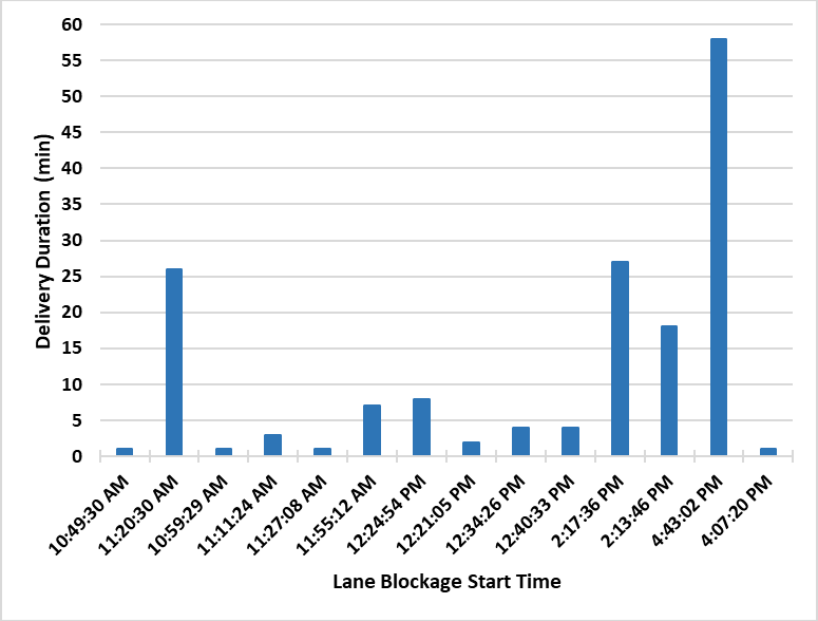

Figure 5: Delivery Duration vs. Time

Figure 6 shows a histogram of the duration of observed lane-blocking delivery events. The distribution shows that double-parked deliveries of less than 6 minutes were the most frequent. However, much longer duration events occurred including one delivery that blocked a lane for nearly 1 hour. The average double-parked delivery duration of the observed set was 12 minutes with a standard deviation of 16 minutes.

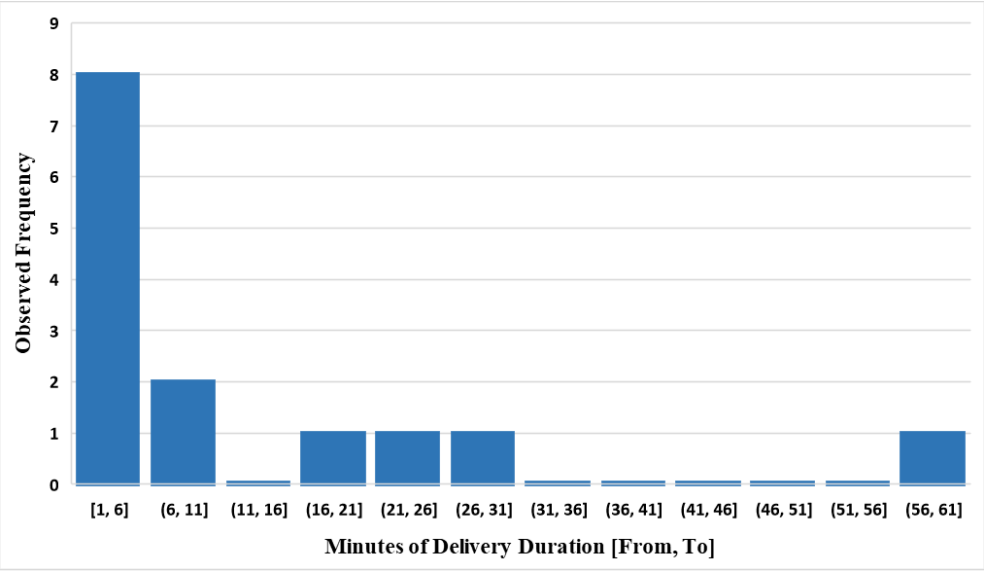

Figure 6: The Distribution of Observed Delivery Durations on 8th Ave

It was confirmed through observation of the 8th Ave data that vehicles will indeed use available lane space downstream of double-parked deliveries to exit the street segment. Six examples of observed deliveries where vehicles merged into the lane downstream of the double-parked delivery vehicle are listed in Table 2. The six observed deliveries in Table 2 where selected because these observation cases did not have a simultaneous lane-blocking delivery occurring in the downstream lane of the downstream street segment. The remaining 8 observations of double-parked delivery cases had simultaneous deliveries occurring downstream that could have discouraged vehicles from using the lane or in any case would have made for a dissimilar comparison with the 6 cases listed in Table 2.

Table 2: Downstream Lane Use by Arriving Vehicles During Double-Parked Deliveries

Observed Delivery Case	1	2	3	4	5	6
Double-Parked Delivery Distance from Stop Line	63ft	65ft	70ft	90ft	100ft	144ft
Side of Street for Blocked Through Lane	Right Side	Right Side	Left Side	Left Side	Left Side	Right Side
Delivery Start Time	1:51 PM	11:08 AM	11:26 AM	11:48 AM	12:19 PM	12:36 PM
Duration (mins)	8.32	3.07	1.37	7.03	1.75	4.43
Total Arrival Flow Rate During the Delivery Period (veh/hr)	1,565	1,096	1,796	1,314	2,091	1,734
No. of Vehs Arriving in the Blocked Lane Downstream of the Delivery Vehicle (veh)	11	3	10	20	13	11
Flow Rate of Vehicles Arriving in Blocked Lane Downstream of the Delivery Vehicle (veh/hr)	79	59	438	171	549	132

As Table 2 shows, in each case where an isolated lane blocking delivery occurred leaving lane space open downstream, vehicles flowed through the open downstream portion of the blocked lane.

2.3 Observed Delay Analysis of Double-Parked Deliveries

An attempt was made to determine the observed difference in delay caused by the 6 isolated double-parked delivery cases listed in Table 2. These deliveries were chosen for analysis because there were no simultaneous deliveries on 8th Ave while they occurred. For each delivery case, a baseline period was chosen for comparison. Typically, the baseline period was chosen as the nearest 15 min period before or after the delivery event when no other deliveries or incidents occurred. In many cases, finding a nearby baseline period was challenging because of frequent deliveries or incidents. Observing the delay during the delivery cases was made challenging by the relatively short duration of the suitable delivery casts, the longest was just over eight minutes. The baseline periods and delivery periods typically have different arrival volume rates. Unfortunately, the nature of the dynamic location on 8th Ave did not easily allow for the exact delivery traffic conditions to be observed without the delivery taking place for comparison.

Observed delay was calculated using a key stroke event recorder manually operated while viewing the video at normal speed. The method creates a time log of vehicle arrivals and departures for each lane from which signal control delay is calculated using the length and duration of vehicle queues. The delay results for each lane are then aggregated for the approach weighted by lane volume. Observed delay was recorded for both baseline and delivery periods, the results are listed in Table 3. The delay refers to the aggregate approach delay on 8th Ave between 36th and 37th streets.

Table 3: Observed Delay: Baseline vs. Delivery

Delivery Case	Delivery Location (ft)	Delivery Duration (min)	Baseline Arrival (veh/hr)	Baseline Delay (sec/veh)	Delivery Arrival (veh/hr)	Delivery Delay (sec/veh)
Case 1	63	8.32	1,484	17.3	1,565	15.1
Case 2	65	3.07	1,430	14.6	1,096	21.9
Case 3	70	1.37	1,430	14.6	1,796	23.9
Case 4	90	7.03	1,212	31.8	1,314	22.2
Case 5	100	1.75	1,428	34.8	2,091	11.1
Case 6	144	4.43	1,575	33.4	1,734	32.2

Table 3 shows contradictory trends. For example, in Delivery Case 1 the arrival volume during the delivery was higher than the baseline period, yet the observed delay during the delivery was found to be less than that during the baseline period. This indicates that the individual lane saturation flow rates were volatile between the observed baseline and the delivery periods likely due to other traffic flow perturbations. Volatile saturation flow rates at the downstream intersection were likely caused by the variability of the effect of pedestrian crossings on turning vehicles, and random queue spill back from the downstream street segment north of 37th Street. Cyclic oversaturation was not observed on 8th Ave, however many random and brief queues occurred downstream of the segment under analysis which affected the discharge rate of the segment under analysis.

In summary, this study was not successful in isolating the empirical delay impact of double-parked deliveries using video data. The example of 8th Ave in Manhattan had the advantage of providing many examples of double-parked delivery vehicles and demonstrating that vehicles will in fact use lane space left open downstream of a delivery vehicle. However, the traffic flow data proved too noisy in other causes of delay variability preventing a meaningful comparison between baseline and double-parked delivery cases.

As a proxy for empirical data, we use microsimulation to isolate the delay impact of double-parked deliveries on 8th Ave. However, first we present two analytical models for estimating the capacity and delay impacts of double-parked delivery vehicles: in Chapter 3, a simple attempt at imitating the existing methodology in the HCM6, then in Chapter 4, a more detailed model consistent with kinematic wave theory. After comparing the two models on a simple two-lane street in Chapter 5, we will return to the 8th Ave example and compare the proposed analytical models to microsimulation in Chapter 6.

CHAPTER 3

AN ALL-OR-NOTHING MODEL

3.1 Capacity for a Two-Lane Street

In this section, a simple model is presented based on the existing HCM6 methodology for incorporating parallel parking maneuvers and buses stopping in a lane on the signalized control delay of an urban street segment. The model is explained using the theoretical two-lane street from Section 1.4.6. As described in Section 1.4.2, parallel parking maneuvers and stopped buses are treated as events that eliminate an entire travel lane for use while they occur. The saturation flow rate of the lane group is reduced for the whole analysis period based on the number of lane blocking events by using the adjustment factors in eqs. 1 and 2. We present a similar method for incorporating a double-parked delivery vehicle. We call this method an All-or-Nothing model, because depending on the location of the delivery, the blockage is either treated as eliminating the saturation flow rate of the lane while the delivery occurs, or as having no effect.

In the HCM6, buses are assumed to reduce the saturation flow rate of a lane to zero when a bus is stopped in the lane located within 250 ft (76.3 m) upstream or downstream of an intersection. This analysis focuses only on the effect of delivery blockages on the street segment where the delivery is taking place, therefore only the distance between the delivery vehicle and the downstream intersection is specified. Rather than use a constant threshold distance, we propose to define the threshold in terms of the maximum length of the queue that can be served by the lane group when the intersection is at saturation, a distance defined in Section 1.4.6 as x_{gmax}.

Figure 7 provides an illustration of the All-or-Nothing model assumption of vehicle behavior while a double-parked delivery vehicle occupies the shared right-turn lane. The distance $x_{D,}$ is measured to determine if the location of the delivery vehicle is close enough to the

intersection stop line to cause a reduction in the saturation flow rate of the shared right-turn lane, *Ssr*.

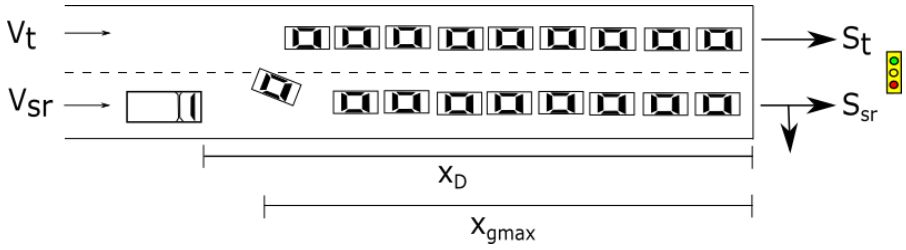

(a)

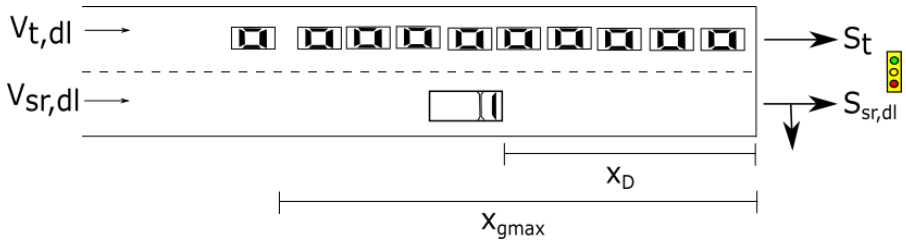

(b)

Figure 7: The All-or-Nothing Model During a Lane-Blocking Delivery

When x_D is less than x_{gmax}, the saturation flow rate of the shared through and right turn lane is adjusted resulting in a new saturation flow rate for the shared-right turn lane, labeled $S_{sr,dl}$ in part b of Figure 7. The reduced saturation flow rate $S_{sr,dl}$ results in a rebalancing of the lane group arrival volumes on the segment $V_{t,dl}$ and $V_{sr,\,dl}$.

A double-parked delivery adjustment factor for saturation flow rate is given by the equation:

$$f_{dl} = \frac{(1 - t_d/T)}{N} \tag{19}$$

where f_{dl} is the delivery blockage adjustment factor, t_d is the duration of the delivery blockage, T is the duration of the analysis period, and N is the number of lanes in the lane group.

The capacity, c_{sr} ,of the shared right-turn lane group in Figure 7 is then also dependent upon the location of the delivery as shown by the equations:

$$c_{sr} = \begin{cases} S_{sr}g/C, \text{if } x_D \geq x_{gmax} \\ S_{sr,dl}g/C, \text{if } x_D < x_{gmax} \end{cases} \quad (20)$$

and

$$S_{sr,dl} = S_{sr}f_{dl} \quad (21)$$

where all other variables are as previously defined. When the delivery blockage location is equal to or upstream of x_{gmax}, the capacity c_{sr} is the unblocked capacity of the lane group.

3.2 Delay for a Two-Lane Street

The All-or-Nothing model creates an adjusted saturation flow rate for the lane group experiencing a delivery blockage which is constant throughout the analysis period. This makes it possible to calculate the uniform control delay of lane groups that do not allow permitted turns using eqs. 10, 11, and 12. substituting the delivery adjusted capacity and arrival rate. Similarly, the incremental delay can be found using eqs. 17 and 18.

Figure 8 shows an example of a before and after QAP diagram for a lane group adjusted with the All-or-Nothing model. The adjusted delivery case is shown by the solid lines, while the non-delivery case is overlaid with dashed lines. The arriving demand $q_{sr,dl}$, which is in units of veh/sec, is a lower arrival rate compared to the non-delivery rate q_{sr} because the reduced saturation flow rate of the lane group, $S_{sr,dl,}$ causes the service time of the lane group to increase, thereby changing the arrival rate equilibrium of through movement vehicles with adjacent lanes. Delay is calculated from the geometry in the QAP diagram in the delivery adjusted case using eq. 16 with the delivery adjusted slopes of the QAP diagram.

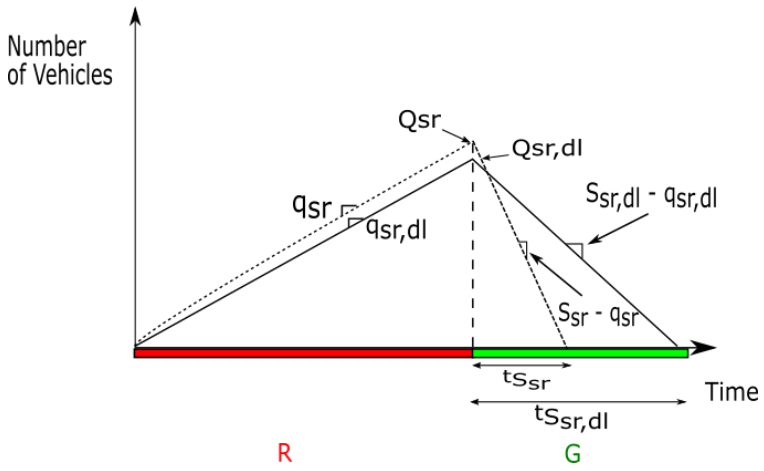

Figure 8: A QAP Diagram Before and After Delivery Blockage Adjustment Using the All-or-Nothing Model

The All-or-Nothing model presented here fits in with the existing HCM6 methodology because it makes similar assumptions about the effect of a lane blockage on the saturation flow rate of a lane group. Furthermore, the delivery blockage adjustment factor, f_{dl}, results in a reduced saturation flow rate for the lane group that is applied to the whole analysis period as a blockage time weighted average which is in keeping with the parallel parking maneuver factor and bus stopping factor from the HCM6.

To represent the dynamics of what occurs when vehicles use the lane capacity downstream of a delivery blockage, as was observed in Chapter 2, a more detailed analytical model is needed. In the next section we present a detailed analytical model to address the shortcomings of the All-or-Nothing model.

CHAPTER 4

A DETAILED ANALYTICAL MODEL

During a double-parked delivery event on an urban street, the All-or-Nothing model described in Chapter 3 eliminates the capacity of the entire travel lane where the delivery vehicle is double-parked for the duration of the delivery event. However, observations of double-parked delivery vehicles in Chapter 2 showed that lane capacity downstream of the double-parked delivery is in fact used by other vehicles on the street segment.

To more realistically model the traffic dynamics around a double-parked delivery vehicle, we present a new analytical model, the Detailed model, informed by kinematic wave theory. The simple two-lane street from Chapter 3 is used to demonstrate the Detailed model in this chapter.

4.1 Capacity for a Two-Lane Street

Considering the simple two-lane street with a double-parked delivery vehicle blocking the shared-right lane, several additional variables are needed to describe the saturation flow rate of lane groups affected by the delivery blockage. Part a of Figure 9 shows non-delivery conditions on the two-lane theoretical street where the back of the queue location, $x_{BQ,sr}$, is the furthest point back from the stop line that the queue in the shared right-turn lane reaches for a given flow rate, v_{sr}.

In part b of Figure 9, we see the Detailed model implied vehicle behavior around a double-parked delivery vehicle located at a distance, x_D, from the stop line. The vehicles use the storage space in the shared right-turn lane between the stop line and the double-parked vehicle. The dimension, W_Φ, is labeled representing the minimum unblocked width between the delivery vehicle and the other side of the bottleneck. The Detailed model characterizes the minimum width, W_Φ, as a bottleneck width located a distance, x_D, from the stop line. The exact definition of W_Φ in a general sense is a matter for further refinement, but for this example, W_Φ is assumed as

equal to the width of the remaining open through lane on the street assuming that the shared-right turn lane is completely blocked.

Part c of Figure 8 illustrates that the portion of the street downstream of the delivery vehicle consisting of unblocked lanes of a length, x_D. This portion of the street stores vehicles that will discharge at flow rates S_t and S_{sr} from each lane respectively. Only the vehicles stored downstream of the delivery vehicle will discharge at these rates.

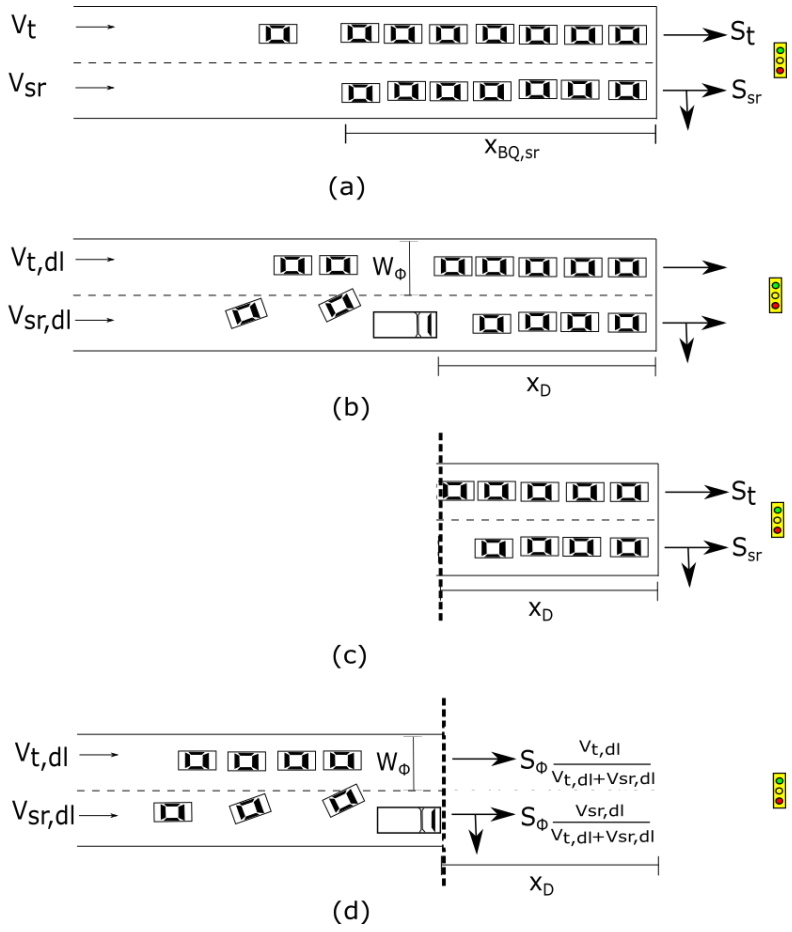

Figure 9: The Detailed Model Saturation Flow Rates with a Double-Parked Delivery Vehicle

Part d of Figure 8 depicts the portion of the street behind the delivery vehicle bottleneck. The arriving traffic must merge to travel through the unblocked cross section of width, W_Φ. The bottleneck has a saturation flow rate of its own, S_Φ. The saturation flow rates of lane groups

downstream of the bottleneck are now constrained by S_Φ and furthermore by the fact that more than one downstream lane group must share the saturation flow rate through the bottleneck. Therefore, the saturation rate for the shared right-turn lane group during a delivery is given by:

$$S_{sr,dl} = \begin{cases} S_{sr}, & for\ vehicles\ queued\ at\ locations\ x\ <\ x_D \\ s_\Phi \frac{v_{sr,dl}}{v_{t,dl}+v_{sr,dl}}, & for\ vehicles\ queued\ at\ locations\ x\ \geq\ x_D \end{cases}. \quad (22)$$

For the adjacent through lane group, the saturation flow rate, $S_{t,dl}$, follows from eq. 22 with the exception that the subscripts *sr* and *t* are replaced with one another in every instance.

It is required to know the expected arrival rates $v_{sr,dl}$ and $v_{t,dl}$ before applying eq. 22. These values can be found by starting with an initial value for each lane group saturation flow rate and then using the results of the first iteration as an input to balancing the arriving through moving vehicles until there is a service time equilibrium among through moving vehicles across lane groups. This iterative process is outlined in a general sense in Chapter 31 of the HCM6.

For lane groups affected by the delivery blockage, the first iteration saturation flow rates should reflect the maximum discharge possible for vehicles occupying a distance, x_D , in the lane group, followed by a discharge from the bottleneck for the remainder of the green time, if any. For the shared right-turn lane on the simple two-lane street this would be:

$$S_{sr,dl_1} = \left(\frac{min(g, t_{x_{D,sr}})}{g}\right) S_{sr} + \left(\frac{\max(g - t_{x_{D,sr}}, 0)}{g}\right) S_\Phi \frac{S_{sr}}{S_{sr} + S_t} \quad (23)$$

where S_{sr,dl_1} is the initial saturation flow rate used during the arrival volume balancing procedure, and $t_{x_{D,sr}}$ is the time it would take to clear vehicles stored in front of the delivery vehicle in a queue of length x_D. The time $t_{X_{D,sr}}\ is$ given by:

$$t_{x_{D,sr}} = \frac{x_D k_j}{S_{sr}} \quad (24)$$

where k_j is the vehicle jam density for the street. Subsequent iterations of the arrival volume balancing procedure would then replace $\frac{S_{sr}}{S_{sr}+S_t}$ with $\frac{v_{sr}}{v_{sr,dl_i}+v_{t,dl_i}}$ in eq. 23 using volumes from the previous iteration until arrival rate equilibrium is reached across lane groups. The through lane group in the example two-lane street would follow a simultaneous process for determining arrival flow rate but the subscripts *sr* and *t* in eqs. 22 and 23 would be transposed in every instance.

Now that the two possible saturation flow rates for lane groups affected by the double-parked delivery have been established, the capacity of the lane groups can be defined. The problem is now to determine how long the intersection can discharge vehicles that are queued downstream of the delivery vehicle and how much time remains to discharge vehicles queued upstream of the delivery vehicle.

The duration of flow from the queue downstream of the intersection at the first saturation rate, t_{sr}, will be limited by the minimum of four possible values which must be checked, they are: 1) the time it takes to serve the queued vehicles if the space between the stop line and the parked delivery vehicle at a distance, x_D , is filled with queued cars, previously defined in eq. 24 as $t_{x_{D,sr}}$, 2) the time it takes to serve the maximum length of queue that is possible to develop in the lane given the effective red time, the arrival rate through the delivery bottleneck, and the queue service time of the lane group, given as:

$$t_{R,S_\Phi} = \frac{(C-g)S_\Phi \frac{q_{sr,dl}}{(q_{t,dl}+q_{sr,dl})}}{max\left\{S_{sr} - S_\Phi \frac{q_{sr,dl}}{q_{t,dl}+q_{sr,dl}}, 1\right\}}, \tag{25}$$

where the arrival flow is labeled $q_{sr,dl} = v_{sr,dl}/3600$, which converts the units of arrival flow rate to veh/sec, 3) the time it takes to serve the maximum queue if the arriving traffic in one or more adjacent lanes develops a queue during arrival that prevents flow through the bottleneck and therefore limits the size of the queue in the lane under analysis, given as:

$$t_{q_t} = \frac{\left(\frac{x_D k_j}{q_{t,dl}}\right) q_{sr,dl}}{S_{sr}}, \tag{26}$$

and 4) the length of the effective green time, g.

After the queue in front of the bottleneck is served, the remaining portion of the effective green time serves vehicles at the second saturation flow rate of the lane group. This remaining time interval, t_{Φ}, is found by subtracting the time required to clear the queue in front of the bottleneck from the effective green time. Finally, the capacity of the shared right-turn lane is given by:

$$c_{s_{sr,dl}} = \frac{1}{C}\left(t_{sr}S_{sr} + t_{\Phi}S_{\Phi}\frac{q_{sr,dl}}{q_{t,dl} + q_{sr,dl}}\right) \tag{27}$$

where

$$t_{sr} = min\{t_{x_{D,sr}}, t_{R,S_{\Phi}}, t_{q_t}, g\} \tag{28}$$

and

$$t_{\Phi} = g - min\{max\{t_{sr}, t_{st}\}, t_{R,S_{\Phi}}, g\} \tag{29}$$

The distinction between t_{sr} an t_{st} in eq. 29 is important in order account for the possibility that the queues in front of the delivery vehicle clear at different times. For example, in the event of a dominant turning movement discharge queue blocking through vehicles at the bottleneck. Using eqs. 27, 28, and 29, the capacity of the through lane in part b of Figure 9 follows from the same calculation, except that the subscripts *sr* and *t* are reversed in every instance.

4.2 Delay for a Two-Lane Street

There are two important distinctions between the Detailed model the All-or-Nothing model regarding delay. First, in the Detailed model, it is no longer possible to use the capacity to calculate uniform control delay with eq.10 because the queue is now served at two different rates during two distinct time intervals within a cycle. Second, the total delay during an analysis period

is calculated by averaging together the delays associated with blocked and unblocked cycles rather than calculating a single average capacity and calculating a delay based on the average capacity.

In the Detailed model, a double-parked delivery vehicle will not increase uniform control delay over the unblocked case unless the arriving volume exceeds the saturation flow rate at the bottleneck location or the location of the delivery vehicle interferes with the back of the queue location, x_{BQ}, in unblocked conditions. The former case would result in a persistent bottleneck queue spillback at the delivery vehicle and will not be addressed in this analysis. The latter case implies that when the bottleneck can accommodate the arrival volume demand, increased uniform control delay is dependent upon the relationship between the location of the delivery vehicle, the traffic arrival rate, and the signal timing.

The queuing delay can be accounted for with a QAP diagram that is constructed for each lane group. Figure 10 shows an example for the shared right-turn lane group of the simple two-lane street. The clearance of the queue during the green phase depends on the durations t_{sr} and t_{Φ} as calculated in eqs. 28 and 29. The area of the polygon provides a measure of the uniform control delay associated with the intersection during freight delivery blockage following the general form of the QAP calculation from eq. 16.

As for incremental delay, the volume to capacity ratio for each lane group, as calculated using the detailed model, is input in to eq. 17 for incremental delay during the blocked cycles. If an analysis period consists of blocked and unblocked cycles, the incremental delay for the analysis period would then be a weighted average of the two types of cycles based on the number of each in the analysis period.

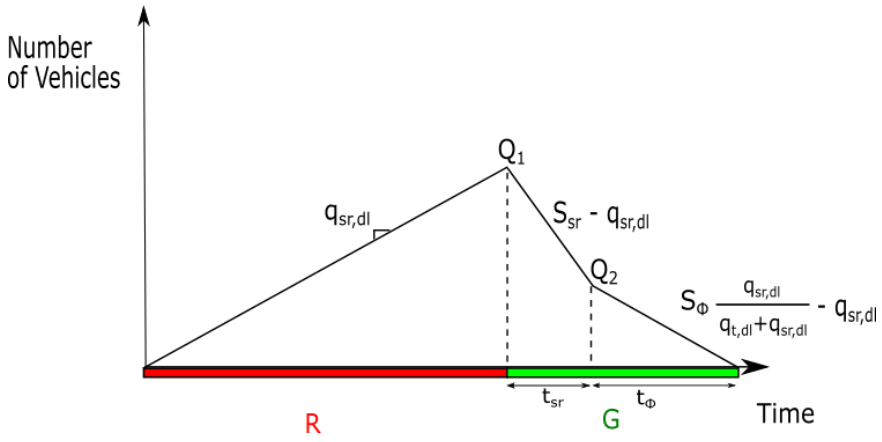

Figure 10: A QAP Diagram for the Detailed Model During a Blocked Cycle

CHAPTER 5

COMPARISON OF ANALYTICAL MODELS ON A TWO-LANE STREET

The modeling approaches presented in Chapters 3 and 4 provide different ways to estimate capacity and control delay on a signalized urban street when a double-parked delivery vehicle blocks a lane. Thus far we have described how to calculate capacity and delay using the All-or-Nothing and the Detailed models, in this chapter we will look at the behaviors of the two models when applied using the two-lane theoretical street from Chapters 3 and 4.

5.1 Comparison of Capacity

For the two-lane theoretical street of Chapters 3 and 4 with one through lane and one shared right-turn, Figure 11 shows a plot of the capacity versus delivery distance using eqs. 20 and 27.

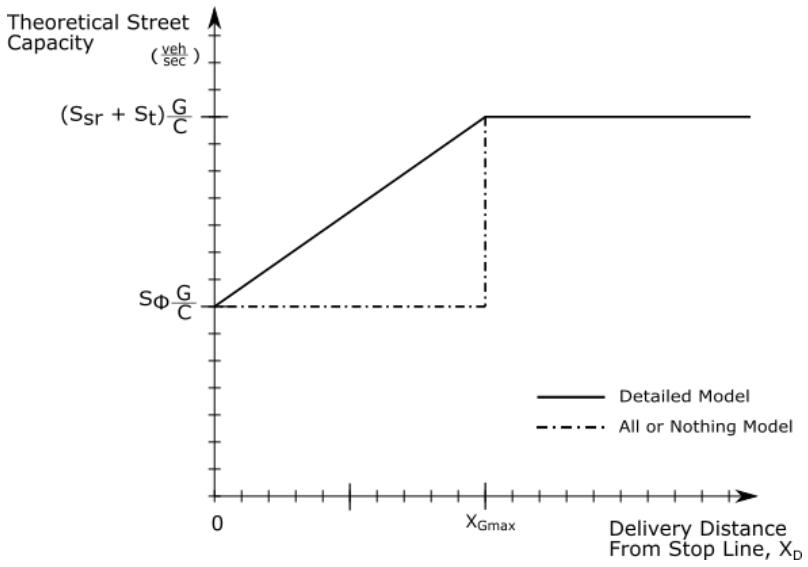

Figure 11: Capacity During a Blocked Signal Cycle Using the Two Modeling Methods

The distinct difference is that the All-or-Nothing model is binary; for a delivery closer to the intersection than x_{gmax} a single reduced capacity value is given reflecting the capacity of the

bottleneck only. The Detailed model shows that the capacity increases gradually as the location of the delivery moves away from the intersection. In theory, for deliveries located further upstream from the intersection than x_{gmax} both models show that the stopped vehicle has no effect on intersection capacity. Driver willingness to use the space in front of the delivery vehicle may prevent this from being so, as would any frictional effect on capacity that the mere presence of the delivery vehicle may have on driver behavior.

These models can be interpreted as bounds for the capacity of the street during a signal cycle when a vehicle delivery is being made. The All-or-Nothing model provides a lower bound, by assuming that the shared right-turn lane group is completely blocked during the delivery. The Detailed model provides an upper bound, by assuming that vehicles fully utilize the street space in front of the delivery vehicle. Actual driver behavior may result in an observed capacity somewhere between these two bounds.

5.2 Comparison of Delay

A numerical example is used to provide a comparison between the control delay estimated using the two methods. The input parameters and critical values for the numerical example are summarized in Table 4. The numerical example uses the same simple two-lane street presented in Chapters 3 and 4.

First, we consider the uniform control delay alone. When there is no delivery on the link, the average vehicle delay is 9.9 seconds per vehicle at the intersection based on eq.10. This is the baseline uniform delay against which the delay during a double-parked delivery is compared.

Table 4: Input Parameters for the Numerical Example Two-Lane Street

Variable Value Units	
Cycle Length	60 sec
Effective Green	30 sec
Total Arrival Rate	900 veh/hr
Number of lanes, N	2
Jam Density, k_j	264 veh/mi
Baseline Saturation Flow Rate for Shared Right-Turn Lane, S_{sr}	1,834 veh/hr
Baseline Saturation Flow Rate for Exclusive Through Lane, S_t	1,900 veh/hr
Saturation Flow Rate at Delivery Vehicle, S_Φ	1,900 veh/hr
Street Length	400ft
Baseline Length of Queue at Saturation, x_{gmax}	317 ft *
Baseline Length of Queue at arrival rate, x_{BQ}	101 ft **
Analysis Period, T	15min

*x_{gmax} is controlled by the through lane in this case, ** x_{BQ} is also controlled by the through lane in this case.

Looking at a single signal cycle while a delivery is occurring, Figure 12 shows how the uniform control delay per vehicle relates to the location of the stopped delivery vehicle for the All-or-Nothing model and the Detailed model. Like the capacity estimates, the models are only in agreement when the delivery vehicle is at the intersection stop line or further upstream than x_{gmax}. The curve of the Detailed model shows how delays diminish as the distance from the intersection to the delivery vehicle, x_D, increases. The Detailed model predicts that when the delivery vehicle is parked upstream of x_{BQ}, the uniform control delay returns to the baseline level.

When looking only at a single cycle during which a freight delivery blocks part of the street, the All-or-Nothing model provides a conservative worst-case estimate of uniform control delay, while the Detailed model shows that the actual uniform control delay may in fact be much less.

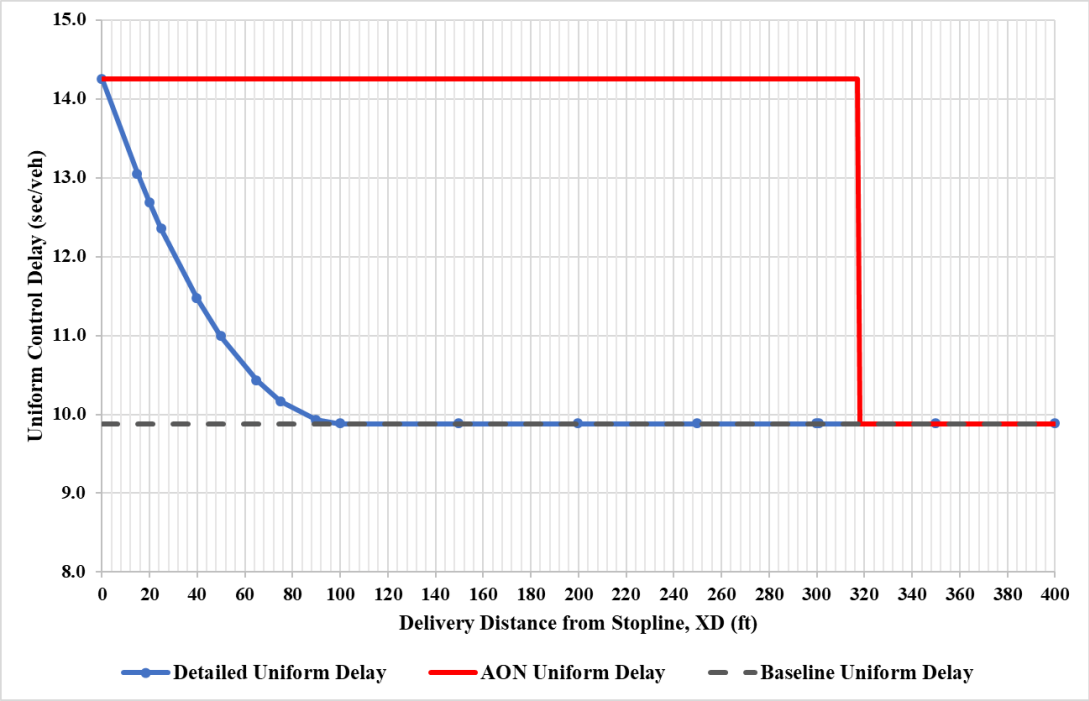

Figure 12: Uniform Control Delay During a Blocked Signal Cycle Using the Two Modeling Methods

A plot of total control delay, which includes the uniform control and incremental delays combined, is noticeably different than the comparison of uniform delay. In Figure 13, we see that the total control delay baseline is now 11.6 sec/veh for the unblocked case. The All-or-Nothing model still changes in a binary fashion at x_{gmax} from the baseline delay to a value of 32.7 sec/veh. The Detailed model delay plot is altered in appearance when incremental delay is included. The Detailed model delay now departs from the baseline when a delivery is located at any point closer than x_{gmax} because this is the blockage location where the potential lane capacity begins to decrease. Even if the arrival rate of traffic does not exceed the capacity of the street, the reduced capacity that occurs when a vehicle is closer than x_{gmax} causes an increase in incremental delay.

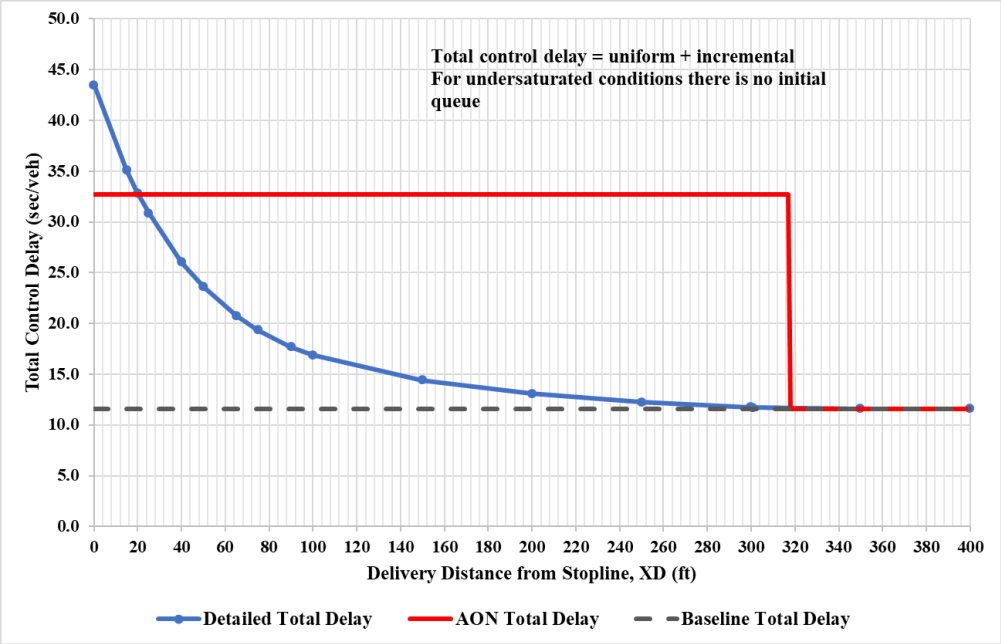

Figure 13: Total Control Delay During a Blocked Signal Cycle Using the Two Modeling Methods

Another notable difference between Figure 12 and Figure 13 is that unlike the uniform control delay plot, the Detailed model now has a higher total delay at the stop line compared to the All-or-Nothing model. This begs the question, how could a delivery vehicle double-parked at the stop line result in more total control delay compared with the elimination of the lane? The reason, in this case, is that the numerical calculation of the Detailed model as presented was not constrained by the following fact: if the delivery vehicle is double-parked at a distance less than one vehicle length from the stop line, no vehicle will be able to use the space downstream of the delivery vehicle. As the capacity of the blocked lane groups decrease with shorter blockage distances to the stop line, the volume to capacity ratios of the lane groups climb. As volume to capacity ratio grows so does incremental delay according to eq. 17. On the theoretical street, the intersection of total delay from the Detailed model and the total delay from the All-or-Nothing model occurs at a delivery distance of 20ft, which corresponds with the assumed vehicle length in the jam density, k_j. Based on this result, it appears that the Detailed model should be constrained to delivery distances greater than one vehicle length from the stop line. In reality, deliveries

closer to the stop line are effectively closing the lane, which would yield a total delay equal to that found in the All-or-Nothing model. The portion of the Detailed model delay plotted above the All-or-Nothing model delay is an artifact which can be derived mathematically but is not possible in reality.

5.3 Comparison of Average Delay During a Partially Blocked Analysis Period

An additional aspect of the delay analysis is to consider how delays caused by blocked lanes are impacted over the course of an analysis period, such as an hour, during which some cycles are blocked, and other cycles are not. The conventional HCM6 approach used for bus blockages and parallel parking maneuvers is to apply a singular average capacity over the course of the analysis period. The delay is calculated by assuming that every cycle in the period has the average capacity. An example of the resulting average uniform control delays are shown by the dashed horizontal lines in Figure 14. The example uses the theoretical two-lane street from earlier delay comparisons. A range of delivery durations in a period of length T = 60 minutes are considered from t_d = 0 (no delivery blockage time) to t_d = 60 minutes (delivery blockage during the whole analysis period).

The calculation of delay based on the average capacity does not accurately reflect the aggregate delay of a partially blocked analysis period. The Detailed model instead requires that the delay be calculated separately for blocked cycles using eq.16 and for the unblocked cycles using eq. 10. A weighted average is then calculated based on the number of vehicles that arrive during the blockage and during the remainder of the period. If the arrival rate is constant, this is the same as using the total duration of deliveries, t_d, as the weight for the blocked delay and the remaining unblocked duration of the period, T-t_d, as the weight for the unblocked delay. The average uniform control delays using the Detailed model are plotted as the solid line curves in Figure 14.

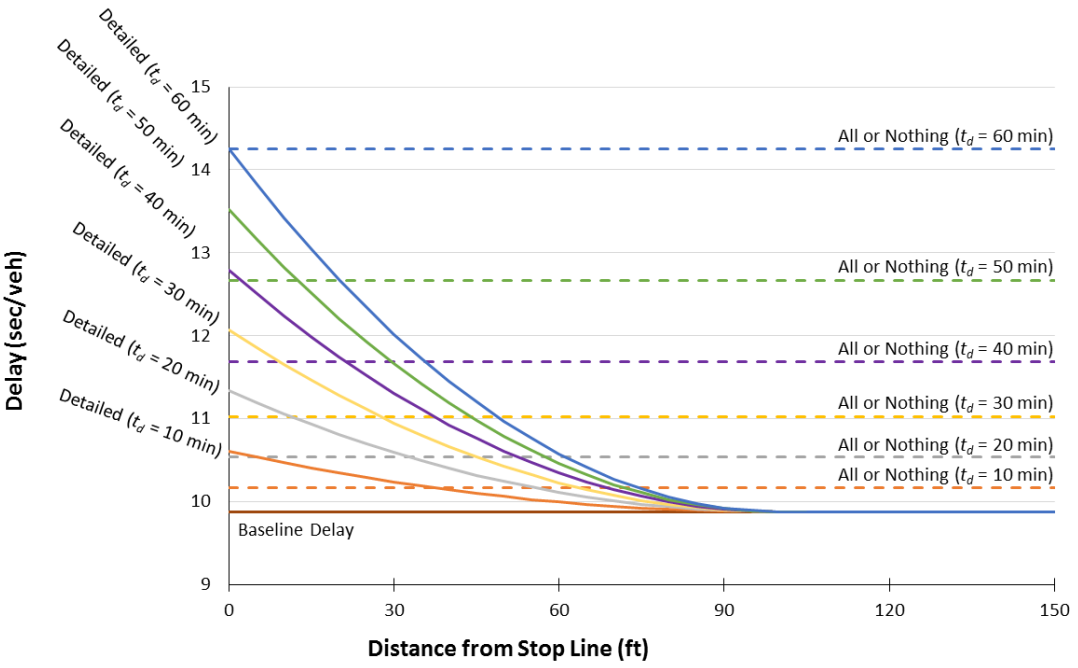

Figure 14: Uniform Control Delay for Different Delivery Durations Within an Analysis Period of 60 Mins

Note that when, t_d=T, the All-or-Nothing model and the Detailed model resemble the uniform control delay comparison for the single blocked cycle in Figure 12. For any delivery duration, t_d, that is less than T, the All-or-Nothing model does not provide the same uniform control delay estimate as the Detailed model when $x_D = 0$. In fact, the simple All-or-Nothing model underestimates the uniform control delay impact of freight deliveries that are close to the intersection and overestimates the uniform control delay impact of deliveries that are further from the intersection. Therefore, the All-or-Nothing model provides neither a conservative or optimistic estimate of delay impacts from freight deliveries; it is a coarse approximation of the actual impacts, which are quantified more precisely by the proposed Detailed model approach. When $x_D = 0$, the error in this numerical example was as much as 10 percent in uniform control delay alone when the duration of the delivery is 30 minutes in an analysis period of 60 minutes.

CHAPTER 6

COMPARISON OF MODEL APPLICATION AND SIMULATION ON 8TH AVE

Returning to the example of 8th Ave in Manhattan first described in Chapter 2, this chapter presents a microsimulation of a segment of 8th Ave and then compares the simulation results with the two analytical models and observed data.

6.1 Simulation Calibration

Because the video capture of 8th Ave focused on the segment of 8th Ave between 36th and 37th streets, the simulation could only be calibrated for that street segment. Still some activity, such as arrival volume turning movements and signals on the downstream segment could be observed from the available vantage point looking north on 8th Ave as shown in Figure 4. A simulation network was constructed and scaled to the correct geometry using an aerial photo from Google Earth. Figure 15 shows the simulation network scope.

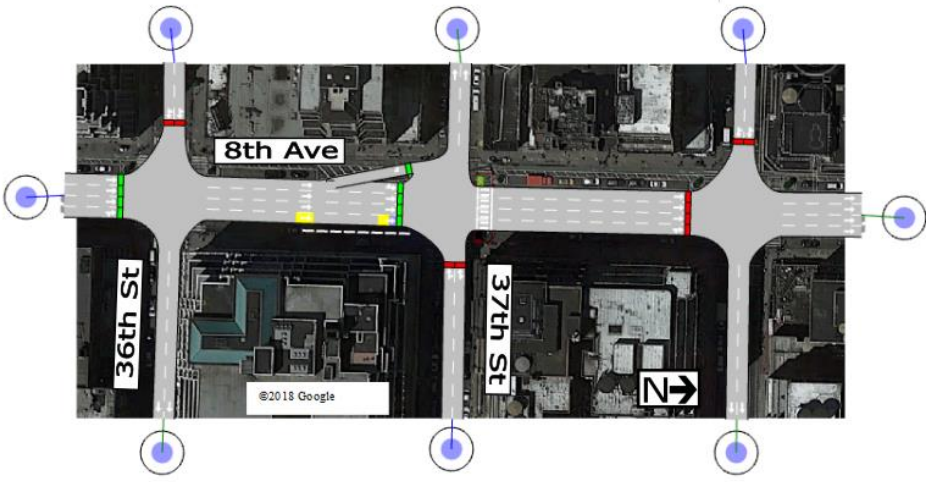

Figure 15: Microsimulation Network of 8th Ave Between 36th and 37th Streets

Before the delivery scenario case could be built, a baseline scenario was constructed to calibrate the simulation based on a delivery-free analysis period. To achieve this, a 13-minute period from 10:55AM to 11:08AM occurring just before the chosen delivery case was analyzed in detail. The 13-minute period, just over 9 signal cycles, was selected because of its proximity in time to the chosen delivery case but also because this was a relatively rare time window that did not have an apparent incident such as another delivery or an emergency vehicle.

During the observed baseline period, arriving traffic to each lane and departure from each lane were recorded manually. A video viewing program was used that allowed for vehicle arrivals and departures from each lane group to be recorded with a manual key stroke. The program produced a time-stamped log for arrivals and departures that was used to keep track of vehicle queues in each lane. The calculation of delay in each lane followed from a record of the number and duration of vehicles in queue. The key result was an estimate of signalized control delay for the approach on 8th Ave between 36th and 37th Streets of 14.6 seconds per vehicle given an observed traffic arrival rate of 1,420 vehicles per hour during the baseline period.

Trip matrices were then created by performing a 15-minute turning movement count, between 11:00AM and 11:15AM for all visible turns in the video. The 15-minute turning movement counts included heavy vehicles and public transit bus stops. At this point, car and truck traffic trip matrices along with a public transit profile could be created based on the turning movement proportions observed from the counts and scaled to the overall traffic arrival rate on 8th Ave as observed in the baseline period.

The baseline simulations were run for 15 minutes in duration and replicated 20 times per scenario. The traffic arrival type was kept on default, which is called Exponential in Aimsun, a Poisson distribution arrival type. For each iteration the resulting approach delay per vehicle on 8th Ave was compared to observed baseline period delay and adjustments were made until the simulation matched the observed baseline period in delay. Calibration adjustments included speed

modifications in some lanes, particularly for turning lanes. Although pedestrian counts were recorded, they could not be simulated due to software license limitations at the volume of pedestrians needed for this Manhattan example. Instead, the turning speeds of vehicles moving through crosswalks were calibrated to match the observed speed of the same turning vehicle movements which frequently had to wait for high volume pedestrian and bicycle crossings.

The calibration was stopped when the simulated approach delay on the 8th Ave segment reached 14.6 seconds per vehicle, the delay from the baseline period. It should be noted however, that the segment delay output report from the simulation only gave a total delay on the segment. Ideally for calibration, the signalized control delay would be isolated from running delay and delay from lane change movements on the link. However, this distinction between sources of delay was not possible to make in the simulation software.

6.2 Delivery Simulation

Now that the simulation was calibrated to an observed baseline of delay, a new set of car and truck trip tables were created to emulate the traffic flow conditions during one of the observed delivery cases. The delivery case selected, Delivery Case 2, occurred at 11:08AM and lasted for just over 3 minutes. The traffic arrival rate during the delivery was 1,096 veh/hr, lower than the baseline period. The observed trip tables made from the turning movement counts were scaled down to equal the delivery traffic arrival rate.

The delivery case location was 65ft upstream from the stop line and parked in the right most through lane. This delivery case was selected because it was one of the observed deliveries that did not have simultaneous deliveries occurring on 8th Ave and vehicles were observed to have used the lane storage space in front of the delivery. Figure 16 shows an image of the delivery simulation running. The software feature used to simulate the parked truck was a so-called traffic incident feature. The square outline appearing in the rightmost lane in Figure 16 is a

defined footprint of a lane blockage that appears for a defined amount of time. The simulated vehicles had to avoid the blocked incident space, emulating a delivery vehicle.

Figure 16: A Snapshot of the Delivery Simulation

An objective of the delivery simulation was to compare the simulated delay to the observed delay during the delivery event. Therefore, the simulation delivery case held the delivery blockage in place for the 15-min duration of the simulation. The purpose of the simulation was not to replicate the observed duration of the delivery within a longer analysis period. Twenty replications were run for the delivery scenario.

The results showed a disparity between delivery effect on delay in the simulation vs. observed. The simulated increase in approach delay went from 14.0 seconds using the delivery arrival rate with no delivery to 14.8 seconds with the delivery. The impact of the delivery blockage was just 0.8 seconds per vehicle in the simulation. It should be noted that the arrival rate of 1,096 veh per hour was well below the capacity of the 4-lane arterial, therefore the small impact on delay was not unexpected.

The observed results from the video showed a much higher delay while the delivery vehicle was present at 21.9 sec/veh. There is no observed delay impact, since the calibration

baseline period had a different arrival rate. Table 5 shows the simulation results for the replication of the selected delivery case.

Table 5: Simulation Results for a Selected Delivery Case

	Intersection Approach Delay (sec/veh)				
Scenario on 8th Ave	**Detailed Model**	**All-or-Nothing Model**	**Simulation Model**	**Simulation 95% Confidence**	**Observed**
No Delivery Baseline for Calibration at 1430 (veh/hr)	14.6	14.6	14.6	+-0.42	14.6
No Delivery at 1096 veh/hr	13.3	13.3	14	+-0.37	Not Available
Case 2 Observed Delivery Event at 1096 (veh/hr) at (x_D=65ft, Right Lane)	13.6	13.9	14.8	+-0.44	21.9
Delivery Delay Impact (sec/veh)	0.3	0.5	0.8		Not Available

Given the disparity between the simulated and observed delivery delays, the analytical models were used to create additional data points of delivery delay impact. Table 5 includes the total control delay values from the Detailed model and the All-or-Nothing model. For the baseline scenario, a spreadsheet equation solver procedure was used to back calculate the saturation flow rate of each lane given the observed arrival flow rate and the observed approach delay. Then, holding the lane saturation rates constant from the baseline case, the delivery case delay values were calculated. The two analytical models were first used to calculate approach delay during the delivery case arrival rate, 1,906 veh/hr, but without a delivery event. Then the delivery case delays were calculated at the same arrival rate. The results show that the two analytical models predicted a change in approach total signalized control delay during the delivery that lower than but more similar in magnitude to the simulation. The Detailed model predicted on 0.3 seconds of delay increase during the delivery, while the All-or-Nothing model predicted 0.5 seconds of

delay. Given that the simulation includes more sources of delay than signalized control delay the lesser impact predicted by the analytical models was expected.

The results of attempting to replicate a single observed delivery case in simulation appeared to show: 1) the simulation resulted in a greater increase in delay than the two analytical methods and, 2) the observed delay during the delivery was much higher than what was predicted by the simulation or the two analytical models. In fact, the observed delay during the delivery, 21.9 sec/veh, was 7.3 sec/veh greater than the observed baseline period delay of 14.6 sec/veh. Given that the baseline period had a significantly higher arrival flow rate, the observed delay value seems flawed. This underscores the findings of Section 2.3 that the observed delay values did not yield meaningful comparisons between baseline and delivery cases most likely due to an inability to isolate the effects of the delivery blockage using a manual observation process on a busy mutli-modal urban street facility.

6.3 Analytical Model Application to 8th Ave: Delay vs. Delivery Location

This section applies the Detailed and All-or-Nothing models to the segment of 8th Ave during lane blocking delivery events at a range of distances from the stop line. Then the delivery simulation scenario from Section 6.2 is used to simulate deliveries at the same range of distances for a comparison of analytical and simulated delay on 8th Ave.

A spreadsheet was created to calculate the signalized control delay of the 8th Ave approach using either the All-or-Nothing model or the Detailed model. The spreadsheet assumed the saturation flow rates derived from the Case 2 baseline period where a known arrival rate produced an observed delay. The arrival rates were borrowed from delivery Case 2 to be consistent with the microsimulation. The spreadsheet included a procedure for balancing the arrival volumes to the lanes that included the effect of delivery location on saturation flow rate and lane arrival allocation as described in Section 4.1. Using the spreadsheet, the uniform and

incremental control delays were calculated for a delivery blockage in the right lane which was placed at a range of distances from the stop line. Figure 17 shows the results for the All-or-Nothing model and the Detailed model.

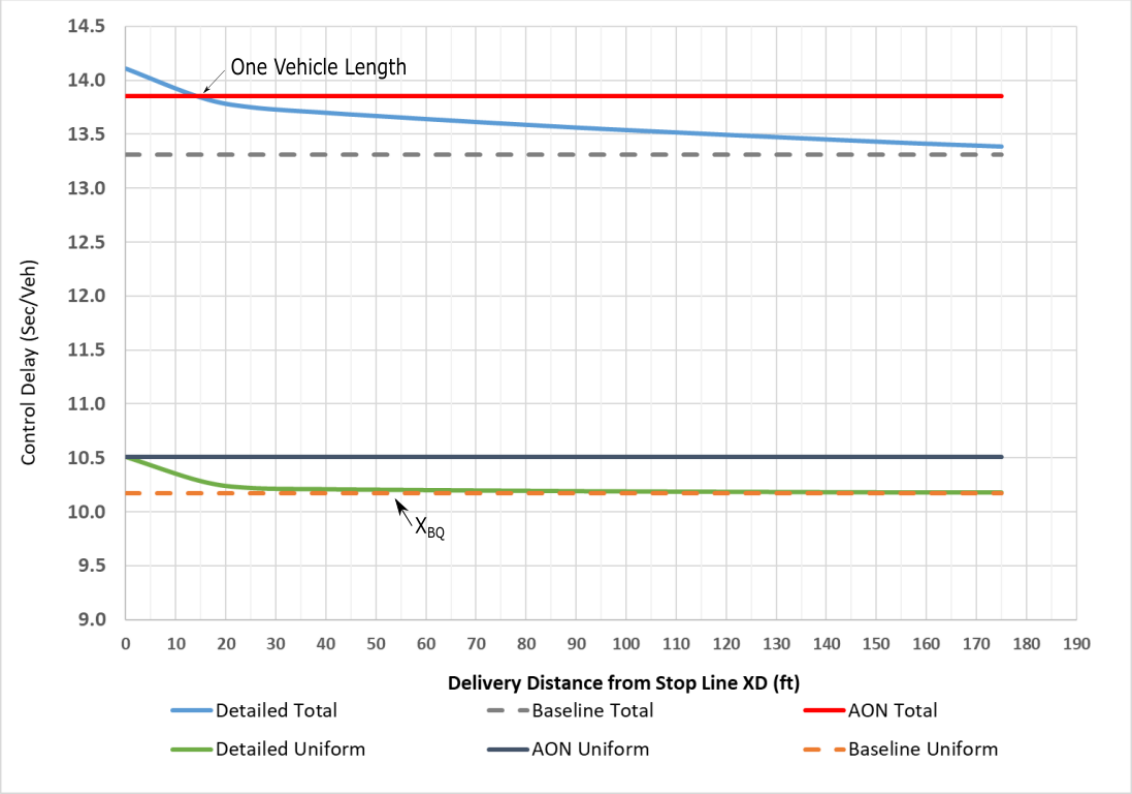

Figure 17: Delay vs. Delivery Distance in the Right Lane of 8th Ave for Two Modeling Methods

Because x_{gmax} is at a greater distance than the length of the street segment, this segment of 8th Ave is treated as losing a lane for any location of a double-parked delivery vehicle according to the All-or-Nothing model. Like the example in Section 5.1, the Detailed model uniform control delay arrives at the same value as the All-or-Nothing model uniform control delay when the delivery is located at the stop line. The Detailed model uniform control delay nearly returns to the no delivery condition at the location x_{BQ}, which was 54 ft for the through lane group in the unblocked condition.

The Detailed model total control delay trend resembles the example using the simple street from Section 5.2 generally. Figure 18 shows a plot of total signalized control delay for the 8th Ave segment between 36th and 37th streets when delivery blockage distances were varied under a total approach arrival rate of 1096 veh/hr.

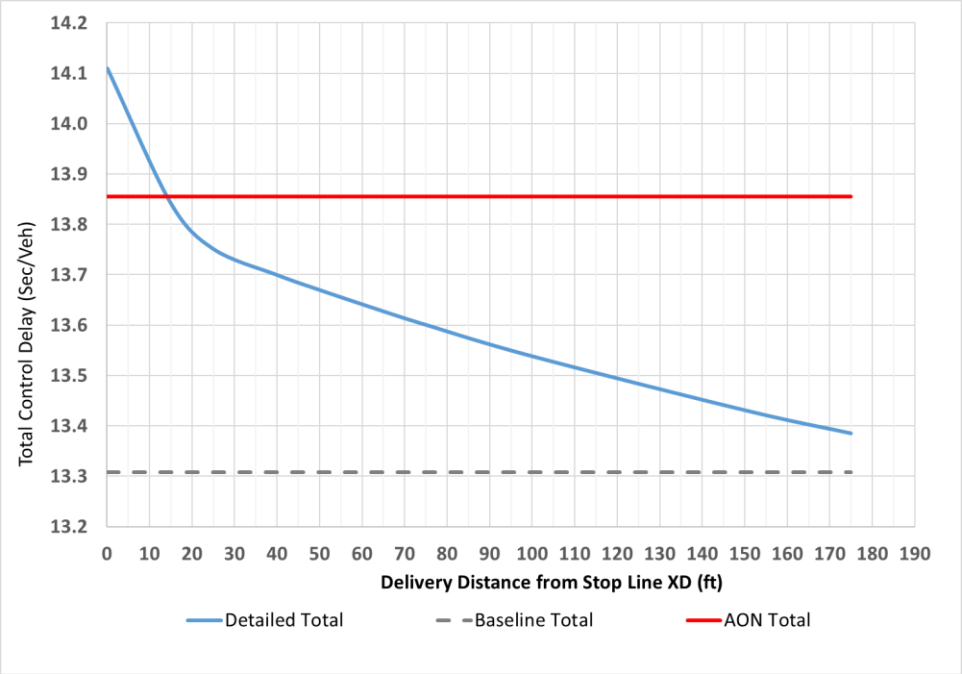

Figure 18: Total Delay vs. Delivery Distance in the Right Lane of 8th Ave Using the Detailed Model

At the stop line, the total control delay exceeds the All-or-Nothing model. However, as discussed in Section 5.2, the All-or-Nothing model total control delay is the practical upper limit because vehicles cannot use the lane at less than one vehicle length. The location where the Detailed model and All-or-Nothing model intersect corresponds to the assumed vehicle length in the jam density, k_j, of the calculations. The Detailed total control delay tapers gradually but does not return to baseline levels because x_{gmax} is at a greater distance than the street length.

6.4 Simulation of 8th Ave: Delay vs. Delivery Location

The microsimulation scenario from Section 6.2 was also used to plot the relationship between delivery distance from the stop line and signalized control delay. The calibration settings from delivery Case 2 scenario were retained. The only parameter that varied for a set of new scenarios was the distance of the delivery blockage from the stop line. One scenario extended the length of the lane blockage to encompass the whole right lane of 8th Ave. This was done to simulate the All-or-Nothing concept of a double-parked delivery. At each delivery distance, a 15-minute simulation was run with the lane blockage present the whole time and twenty replications were run for each scenario. The results of aggregate intersection approach delay for each right lane delivery location scenario are shown in Figure 19. The confidence interval bars displayed are for the 95 percent confidence level.

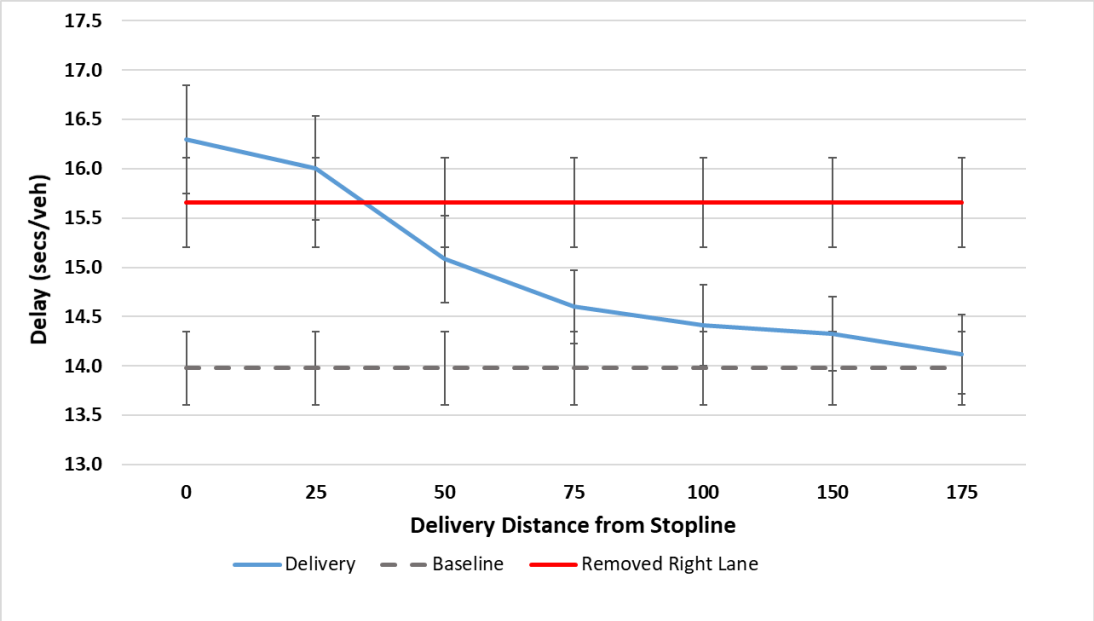

Figure 19: Total Delay vs. Delivery Distance in the Right Lane of 8th Ave Using Simulation

In the results of the microsimulation, the magnitude of the delivery impact on total approach delay was greater than predicted by the Detailed model, 2.3 seconds when the delivery

was located at the stop line vs. 0.8 seconds for the Detailed model. However, the trend of the delivery delay with respect to distance from the stop line does resemble the Detailed model total control delay in Figure 18. Like Figure 18, the simulation delivery delay descends toward but does not quite reach the baseline delay level at 175ft. It should be noted however, that the confidence interval bars between the delivery delay and the baseline delay begin to overlap between 50 and 75 ft, meaning that beginning in that range and further upstream, the difference between the two trend lines could possibly be statistically insignificant at the 95% level.

Like Figure 18, the delivery simulation scenario delay intersects the removed lane scenario delay. However, the cause of the two delay plots crossing is believed to be different in the simulation as compared to the analytical model application. The simulation output attributes on the modeled network give a single value of total delay for a network link that includes all delay experienced by vehicles traveling on the link. In addition to signal control delay, vehicles in the microsimulation experience running delay and delay resulting from lane changes made to avoid the double-parked delivery. It is posited that these additional sources of delay on the link have added a positive vertical offset to each delivery delay data point. If signal control delay could be isolated in the microsimulation or if the other sources of delay normalized for, it is suspected that the signalized control delay during the delivery scenarios would merge with the removed lane scenario at a location point near one vehicle length upstream of the stop line. The additional sources of delay captured in the microsimulation are likely also contributing to the difference in delay impact magnitude between the Detailed model and the simulation results.

The application of the analytical models and microsimulation to 8th Ave in Manhattan showed encouraging initial results that the Detailed model does a reasonably good job of at least emulating the phenomenon of the impact trend that double-parked deliveries will make on signalized control delay at a range of distances from the downstream intersection. This was important to verify before further refinements to the Detailed model can be made.

Even from these initial results, two relevant findings for urban freight policy appear to emerge: 1) double-parked delivery vehicles impact signalized control delay on an urban arterial less when located at a greater distance upstream from the downstream segment intersection, and 2) double-parked vehicles at the intersection stop line have the biggest impact on delay. It would be incorrect however, to conclude that the furthest upstream end of the street segment is the ideal location for a double-parked delivery to occur. This is because a double-parked vehicle at the very rear of a street segment happens to be very near the stop line of the upstream street segment. For this reason, the middle of the street segment is a location that decreases delay impact on the street segment where the delivery is taking place, while also moderating the blockage impact on the stop line discharge of the upstream segment. For a planning scenario in which double-parked vehicles must be tolerated for lack of an alternative, policy that advises delivery makers to prioritize blocking a lane in the mid-block area of the street could minimize delivery delay impact on signalized control delay for other vehicles in traffic.

Furthermore, any program that seeks to identify high impact candidate freight receivers for mitigation, such as an off-hour delivery program should, consider the location on the street where the candidate tends to receive freight. Receivers who routinely attract double-parked deliveries near the stop line of an intersection should be prioritized due to the likelihood that the location of lane blockages caused by the deliveries they receive is most detrimental to the signalized control delay experienced by traffic on the subject arterial.

CHAPTER 8

CONCLUSION

7.1 Summary of Main Findings

Urban freight deliveries are a growing concern in cities around the world as increasing demand for goods deliveries results in increased truck traffic and blockages caused by double-parked delivery vehicles. This study addresses the problem of double-parked urban freight deliveries in urban areas blocking traffic, which reduces street capacity and imposes delays on vehicles. Although urban freight is gaining increasing attention in the literature, there remains a need for methods to quantitatively assess the impact of double-parked delivery vehicles on the performance of signalized arterials.

Currently, the HCM6 does not have any specific recommendations for accounting for urban freight except to account for the heavy vehicle percentage in the traffic stream. The nearest traffic impact that is presented in the HCM6 is to account for lanes that are blocked by buses that stop for passengers. Downstream lane blockage effect on upstream intersections and work zone lane restriction effect on downstream intersections were included in the HCM6 but still leave unanswered questions about double-parked delivery vehicles, particularly regarding the dynamics of traffic flow around them.

A method is developed along the same lines as existing methodology in the HCM6 called the All-or-Nothing model. However, we show that this provides only a coarse accounting of the impact of the freight delivery on capacity and delay.

Video data from a short segment of 8th Ave in Manhattan was shared with the authors by the NYCDOT Office of Freight Mobility[2]. The data captured abundant urban freight activity in a

[2] http://www.nyc.gov/html/dot/html/motorist/trucks.shtml

six-hour period and confirmed that vehicles will indeed use open downstream lane space in front of double-parked delivery vehicles. Attempts at empirical quantification of the impact on signalized control delay of observed double-parked deliveries were not successful because of the difficulty in isolating the impacts of the deliveries from the dynamic traffic multi-modal environment.

An approach that is consistent with the dynamics of queuing on a street segment is presented as the Detailed model. This model is a little more complex than the All-or-Nothing approach, but it still results in closed form analytical formulas for capacity and delay. The results show that the Detailed model can account for characteristics of urban freight deliveries that were observed in the field but not accounted for with the coarse All-or-Nothing model.

Simulation increased the credibility of the proposed Detailed model. Specifically, the trend of signalized control delay in microsimulation looks more like the Detailed model than the All-or-Nothing model as the delivery vehicle double-parked at increasing distances away from the stop line.

The purpose of this paper is to draw attention to the problem of double-parked urban freight deliveries and propose an initial model to quantify the impacts of deliveries on signalized control delay. This model is important, because we need to be able to quantify the effect of freight deliveries on traffic to design appropriate policies and management strategies to deal with the problem. Quantifying the delay impacts of regularly occurring events that may have small individual impacts is important, because these types of events often have a larger impact on annual delay than infrequent events that have large individual delay impacts.

Two policy implications are highlighted at the conclusion of the results: 1) that double-parked deliveries located mid-block on a segment are likely less impactful on the signalized control delay of the subject segment and the upstream segment since mid-block is the most distant location from both upstream and downstream stop lines, and 2) frequent receivers of

double-parked freight deliveries located near an intersection stop line on an arterial should be prioritized as candidates for policies, such as off-hour delivery programs, that seek to mitigate the impacts of urban freight delivery.

7.2 Remaining Questions and Future Applications

Many questions remain concerning refinement of the technical approach of the Detailed model, the application of this research, and validation through empirical data. More extensive analysis with microsimulation and field data collection are necessary to assess how well these theoretical models represent real delay impacts on real city streets.

The Detailed model needs refinement and calibration to address discontinuity when the delivery vehicle is within one vehicle length from the stop line. Additionally, the examination of a frictional effect which may reduce flow through the bottleneck is needed, particularly since the HCM6 now includes frictional modifiers for downstream lane restriction and work zone bottlenecks. The exact definition of the bottleneck width is also a matter needing more research. Also, there may be a need to adjust how much of the available space in front of the delivery vehicle drivers are likely to use. The Detailed model does not include provisions for simultaneous deliveries on a street segment. While the HCM6 now includes a procedure for penalizing the capacity of an upstream intersection when there is a downstream lane blockage, it does not delve into the dynamics of the distance of that blockage to the upstream intersection. The Detailed model could be expanded to find the signalized control delay impacts on two consecutive urban street segments and identify the location of minimum impact on the two-segment system. Based on the results of this research, it is believed that mid-block double-parked deliveries may minimize delay on a two-segment system.

A refined Detailed model could find numerous applications including: signal retiming to optimize control performance during a delivery, safety analyses of double-parked deliveries, the evaluation of curbside delivery location policy, the quantification of double-parked delivery cost

to other road users, the environment, and public health, and reliability analysis for urban street facilities.

A specific example of how a refined Detailed model could be useful in the policy realm is some researchers have investigated the potential of shifting deliveries to off-hours when traffic volumes are lower. The Detailed model could be useful in helping to quantify the value of making that shift in addition to the more often cited impacts of delivery vehicles on congestion during their travel. This technical addition to macro-scale estimates of delivery cost could enhance the ability to identify how much it is worth incentivizing carriers or receivers to change their behavior or identifying which locations and times of day should be targeted for such a program.

To better isolate the delay of a double-parked freight deliveries during empirical data collection, a location with relatively few other traffic perturbations is needed that can be observed for a greater length of time. Alternatively, an automated monitoring solution could analyze dynamic field data and normalize the results to isolate the impact of delivery delay. It's plausible this could be achieved via some combination of delivery vehicle tracking and automated arterial performance monitoring detection.

BIBLIOGRAPHY

1. Eisele, W.L., Schrank, D.L., Schuman, R., & Lomax, T. J. (2013). Estimating urban freight congestion costs: Methodologies, measures, and applications (Report No. 13-1344). Paper presented at the Transportation Research Board 92nd Annual Meeting, Washington, D.C.

2. Schrank, D., Eisele, B., Lomax, T., & Bak, J. (2015). 2015 Urban Mobility Scorecard. College Station, TX: Texas A&M Transportation Institute and INRIX.

3. Benekohal, R.F., & Zhao, W. (2000). Delay-based passenger car equivalents for trucks at signalized intersections. Transportation Research Part A, 34(6):437-457.

4. Ukkusuri, S.V., Ozbay, K., Yushimito, W.F., Iyer, S., Morgul, E.F., & Holguin-Veras, J. (2015).
Assessing the impact of urban off-hour delivery program using city scale simulation models. EURO Journal on Transportation and Logistics, 5(2), 205-230. DOI 10.1007/s13676-015-0079-3.

5. Skabardonis, A., Dowling, R., Kiattikomol, V., & Safi, C. (2014). Developing improved truck passenger car equivalent values at signalized intersections. Transportation Research Record, 2461, 121-128.

6. Dowling, R., List, G., Yang, B., Witzke, E., & Flannery, A. (2014). Incorporating truck analysis
into the Highway Capacity Manual (NCFRP Report 31). Washington, D.C.: Transportation Research Board.

7. Han, L., Chin, S.-M., Franzese, O., & Hwang, H. (2005). Estimating the impact of pickup- and delivery-related illegal parking activities on traffic. Transportation Research Record, 1906:49-55.

8. Kawamura, K., Sriraj, P., Surat, H., & Menninger, M. (2014). Analysis of factors that affect the frequency of truck parking violations in urban areas. Transportation Research Record, 2411, 20-26.

9. Tipagornwong, C., & Figliozzi, M.A. (2015). A study of the impacts of commercial vehicle parking availability on service costs and double parking behavior (Report No. 15-5584). Paper presented at the Transportation Research Board 94th Annual Meeting, Washington, D.C.

10. Zou, W., Wang, X., Conway, A., & Chen, Q. (2016). Empirical analysis of delivery vehicle onstreet parking pattern in Manhattan area. Journal of Urban Planning and Development, 142(2), 04015017.

11. Cherrett, T., Allen, J., McLeod, F., Maynard, S., Hickford, A., & Browne, M. (2012). Understanding urban freight activity—key issues for freight planning. Journal of Transport Geography, 24, 22-32.

12. Ahrens, G.A., Forstall, K.W., Guthrie, R.U., & Ryan, B.J. (1977). Analysis of truck deliveries in a small business district. Transportation Research Record, 637, 81-86.

13. Habib, P.A. (1981). Incorporating lane blockages by trucks in intersection analysis and signal timing. Transportation Research Part A, 15(6), 459-464.

14. Holguin-Veras, J., Wang, Q., Xu, N., Ozbay, K., Cetin, M., & Polimeni, J. (2006). The impacts of
time of day pricing on the behavior of freight carriers in a congested urban area: Implications to road pricing. Transportation Research Part A, 40(9), 744-766.

15. Palmer, A., & Piecyk, M. (2010, September). Time, cost and CO2 effects of rescheduling freight deliveries. Paper presented at the 2010 Logistics Research Network Conference, Harrogate, North Yorkshire, England.

16. Su, F., & Roorda, M.J. (2014). The potential of urban freight consolidation for the Toronto central business district, No. 14-2104. Transportation Research Board 93rd Annual Meeting, January 12-16, Washington, D.C.

17. Fioravanti, R., Guerrero, P., & Chung Cho, E. (2015). Modeling public policies on urban freight distribution: Tackling emissions, congestion, and logistics costs, No. 15-3578. Transportation Research Board 94th Annual Meeting, January 11-15, Washington, D.C.

18. Holguin-Veras, J., Perez, N., Cruz, B., & Polimeni, J. (2006). Effectiveness of financial incentives for off-peak deliveries to restaurants in Manhattan, New York. Transportation Research Record, 1966, 51-59.

19. Holguin-Veras, J., Silas, M., Polimeni, J., & Cruz, B. (2008). An investigation on the effectiveness of joint receiver-carrier policies to increase truck traffic in the off-peak hours: Part II: The behavior of carriers. Networks and Spatial Economics, 8(4), 327-354.

20. Silas, M., & Holguin-Veras, J. (2009). Behavioral microsimulation formulation for analysis and
design of off-hour delivery policies in urban areas. Transportation Research Record, 2097, 43-50.

21. Holguin-Veras, J., Silas, M., Polimeni, J., & Cruz, B. (2007). An investigation on the effectiveness of joint receiver-carrier policies to increase truck traffic in the off-peak hours: Part I: The behavior of receivers. Networks and Spatial Economics, 7(3), 277-295.

22. Crainic, T.G., Ricciardi, N., & Storchi, G. (2004). Advanced freight transportation systems for
congested urban areas. Transportation Research Part C, 12(2), 119-137.

23. Yannis, G., Golias, J., & Antoniou, C. (2006). Effects of urban delivery restrictions on traffic movements. Transportation Planning and Technology, 29(4), 295-311.

24. Holguin-Veras, J., Ozbay, K., Kornhauser, A., Brom, M., Iyer, S., Yushimito, W., Ukkusuri, S.,Allen, B., & Silas, M. (2011). Overall impacts of off-hour delivery programs in New York City metropolitan area. Transportation Research Record, 2238, 68-76.

25. Ukkusuri, S. V., Ozbay, K., Yushimito, W. F., Iyer, S., Morgul, E. F., & Holguin-Veras, J. (2016).
Assessing the impact of urban off-hour delivery program using city scale simulation models. EURO Journal on Transportation and Logistics, 5(2), 205–230.

26. Lighthill, M., & Whitham, G. (1955). On kinematic waves. II. A theory of traffic flow on long crowded roads. Proceedings of the Royal Society of London A, 229, 317-345.

27. Richards, P. (1956). Shock waves on the highway. Operations Research, 4(1), 42-51.

28. Transportation Research Board (2016). Highway Capacity Manual 6th Edition: A Guide to Multimodal Mobility Analysis. Washington, D.C. Transportation Research Board of the National Academies.